Synthesis, Structures and Spectroscopic Properties of Copper and Nickel Complexes with Nitrogen Donor Ligands
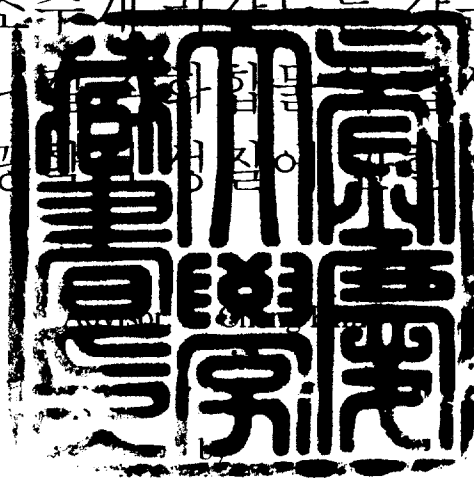
질소중개 리간드를 갖는
구리 및 니켈착물의 성, 구조
및 분광학적 성질에 관한 연구

Jungyun Roh

A thesis submitted in partial fulfillment of the requirements for the degree of
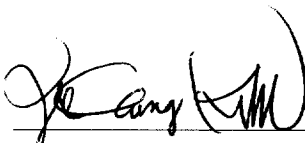Master of Science

in the Department of Chemistry, Graduate School,
Pukyong National University

February 2006

Synthesis, Structures and Spectroscopic Properties of Copper and Nickel
Complexes with Nitrogen Donor Ligands

A Thesis

by

Jungyun Roh

Approved as to style and content by:

_____
Chairman: Don Kim

_____
Member: Yong Cheol Kang

_____
Member: Ju Chang Kim

February 2006

Table of Contents

List of Tables

List of Figures

Synthesis, Structures and Spectroscopic Properties of Copper and Nickel Complexes with Nitrogen Donor Ligands

Jungyun Roh

Department of Chemistry, Graduate School,

Pukyong National University

Abstract

Two new copper(II) complexes of 3,14-dimethyl-2,6,13,17-tetraazatricyclo[14.4.0$^{1\,18}$.0$^{7\,12}$]docosane ligands (L)   have been synthesized and characterized by a combination of analytical, spectroscopic and crystallographic methods. In amber [Cu(L1)]·(ClO$_4$)$_2$ (1), the ligand conformation is planar, and octahedral coordination about the copper ion is completed by two unidentate ClO$_4^-$ ions. In midnight blue [Cu(L2)(O$_2$CH)]·ClO$_4$ (2), the coordination geometry about the copper atom adopts an unusual square pyramid with four equatorial nitrogen atoms from the macrocycle and an oxygen atom from the formate ligand, with an uncoordinated ClO$_4^-$ ion. In both complexes, various types of hydrogen bonding interactions play an important role to produce such geometries around the copper(II) ions.

A bis(μ-oxo)dinickel(III) complex with Me$_4$-pyxyl ligand, which shows the first reactivity of arene hydroxylation by a bis(μ-oxo)dinickel(III) core, has been successfully generated by treating the corresponding bis(μ-hydroxo)dinickel(II) complex with equimolar amount of H$_2$O$_2$ at low temperature. The bis(μ-oxo)dinickel(III) complex exhibits a characteristic UV-vis absorption band at 407 nm and a resonance Raman band at 616 cm^{-1} which shifted to 586 cm^{-1} upon ^{18}O-substitution. Kinetic studies and isotope labeling experiments using H$_2$^{18}O$_2$ imply the existence of intermediate(s) such as peroxo dinickel(II) in the formation process of the bis(μ-oxo)dinickel(III) complex. The bis(μ-oxo)dinickel(III) complex gradually decomposes, leading to arene hydroxylation of the supporting ligand. Isotope labeling experiment indicates the oxygen source of the phenoxo group is H$_2$O$_2$, which shows the arene hydroxylation involves oxygen transfer from the bis(μ-oxo)dinickel(III) core. A similar arene hydroxylation occurred in the Cu system where (μ-η^2:η^2-peroxo)dicopper(II) complex with the same ligand was observed as an intermediate. Comparison of the structure and reactivity of the active oxygen complexes between the Ni and the Cu systems are discussed.

General Introduction

Macrocyclic polyamines and their metal complexes have been the theme of extensive studies for several decades. Macrocyclic compounds are found extensively in nature, playing a role in some important biological processes. Special attention and great efforts have been devoted to the studies of tetraaza macrocycles, because of their potential relationship to the naturally occurring porphyrins and porphyrin-analogs. For examples, the conversion of light energy from the sun into electrical and chemical energy in photosynthesis depends on a magnesium containing macrocycle, chlorophyll, oxygen is transported through the blood by heme, and a vitamin B12 contains a cobalt ion. The naturally occurring molecules are often very complex and difficult to study due to their association with several proteins. One approach used to help understanding the processes is to make the model compounds which have characteristics similar to the molecules found in nature. Model compounds can often provide insight into the important factors of the structure of the naturally occurring complexes as well as giving information into the design of systems which can mimic biological behavior. Thus synthetic tetraaza macrocyclic complexes have been used as model systems for these natural products.

In the meantime, dioxygen activation by transition-metal complexes is one of the most important and attractive research objectives not only in bioinorganic chemistry

but also in numerous and diverse array of catalytic oxidation reactions. Specially, tyrosinase is a ubiquitous binuclear copper enzyme, found in fungi, plants, and animals, that catalyzes the hydroxylation of phenols to catechols and the oxidation of catechols to quinones. To understand the mechanism of tyrosinase, nickel complex with hydrogen peroxide species has also been investigated as mimetic models.

Overall, this thesis is composed of two chapters. In the Chapter I, we report the syntheses and properties of noble Cu(II) complexes with tetraaza macrocyclic ligands. The details of the structures for the new complexes are determined by spectroscopic and X-ray diffraction methods. The works in this chapter were carried out at the Pukyong National University in Korea. In the Chapter II, we describe the synthesis, characterization, and reactivity of the Ni complexes with nitrogen donor ligand. This study was done at the Kanazawa University in Japan under the supervision of Professor Masatatsu Suzuki.

CHAPTER I

Syntheses and Structures of Copper(II) Complexes

Stabilized by Hydrogen Bonding

Abstract

Two new copper(II) complexes of the 3,14-dimethyl-2,6,13,17-tetraazatricyclo[14.4.0^{1,18}.0^{7,12}]docosane ligand (**L**) have been synthesized and characterized by a combination of analytical, spectroscopic and crystallographic methods. Crystal data for amber [Cu(**L1**)]·(ClO$_4$)$_2$ (**1**) at 100 K: monoclinic space group C2/c, a = 19.8962(6), b = 12.5133(4), c = 11.4168(3) Å, β = 114.929(2)$^{\circ}$, V = 2577.58(13) Å^3; midnight blue [Cu(**L2**)(O$_2$CH)]·ClO$_4$ (**2**) at 100 K: monoclinic space group P2(1)/c, a = 8.8005(2), b = 18.6671(4), c = 15.4825(3) Å, β = 96.7040(10)$^{\circ}$, V = 2526.07(9) Å^3. In **1**, the ligand conformation is planar and octahedral coordination about the copper ion is completed by two unidentate ClO$_4^-$ ions. In **2**, the coordination geometry about the copper atom adopts an unusual square pyramid with four equatorial nitrogen atoms from the macrocycle and an oxygen atom from the formate ligand, with an uncoordinated ClO$_4^-$ ion. In both

complexes, various types of hydrogen bonding interactions play an important role to produce such geometries around the copper(II) ions.

1. Introduction

The 14-membered macrocycle, 1,4,8,11-tetraazacyclotetradecane (cyclam, **L3**) is one of the most studied macrocyclic ligands. The introduction of C- or N-substituents on **L3** impacts the structures and reactivities in a variety of transition metal systems. [1-8] The addition of substituents onto the ring generally is reflected by loss of ligand flexibility which is manifested in metal ion complexation behavior that is usually slower relative to **L3**. [9-11] The ligand **L**, containing two cyclohexane rings and methyl groups at the carbon atoms of the macrocycle has been shown to have somewhat different structural properties in several metal complexes when compared with the related metal complexes of **L3**. Many interesting complexes including manganese(III), [12] nickel(II), [13-15] copper(II), [13-15] and zinc(II) [16] ions with **L2** have been prepared and their structures elucidated earlier. As one continuation of the investigation of the transition metal chemistry of **L**, a six-coordinate [Cu(L1)] · (ClO$_4$)$_2$ (**1**) and a five-coordinate [Cu(L2)(O$_2$CH)] · ClO$_4$ (**2**) have been prepared and studied. The copper(II) ion in **1** is coordinated by two ClO$_4^-$

anions at the axial positions, resulting in an elongated octahedral geometry. Each ClO_4^- forms two hydrogen bonds with the macrocyclic ligand at pre-organized binding sites. These binding sites are *trans* to each other on the N4 macrocycle. Reactions of $Cu(OAc)_2 \cdot H_2O$ with **L** followed by sodium perchlorate have been reported before and the square planar $[Cu(L)](ClO_4)_2$ structure has been suggested on the basis of electronic spectral results. [15] However, in the present case the similar reaction procedure using $Cu(ClO_4)_2 \cdot 6H_2O$ instead of $Cu(OAc)_2 \cdot H_2O$ afforded the distorted octahedral complex **1** in the solid state. The coordination environment about the copper(II) ion in **2** is a square pyramid with four nitrogen atoms from the macrocycle and an oxygen atom from the formate ion. Numerous copper(II) complexes with tetraaza macrocyclic ligands have been reported but most of the structurally determined copper(II) complexes are six-coordinate. Five-coordinate copper(II) complexes with tetraaza macrocycles are still rare. The details of the structures of **1** and **2** and the pre-organization of N-H directionality, with its role in profacial selection of anion binding, in **1** are discussed in this report.
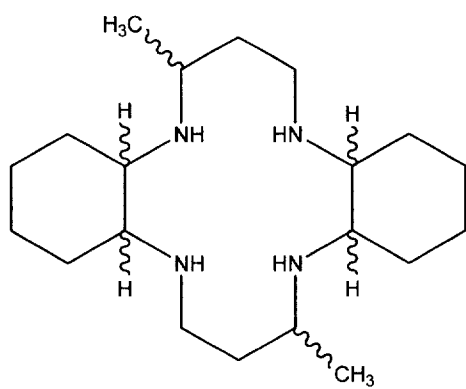
L
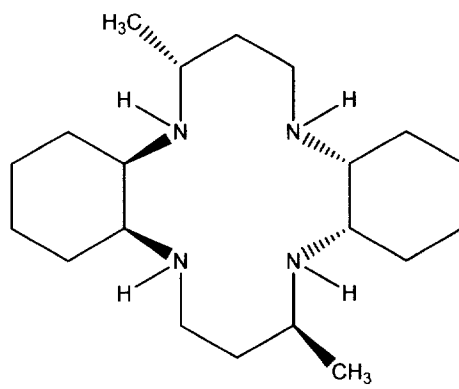
L1
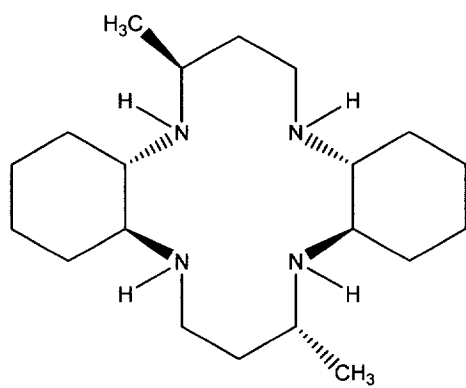
L2
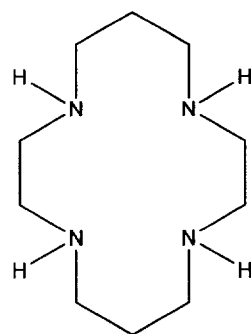
L3

2. Experimental

2.1 Physical measurements

All chemicals utilized in this investigation were obtained from commercial sources as reagent grade, and used without further purification. Distilled water available from in-house resources was used for all procedures. Infrared spectra of solid samples were recorded on a Perkin-Elmer Paragon 1000 FT-IR spectrophotometer between 4000 cm^{-1} and 400 cm^{-1} as on KBr discs method. The analytical laboratory of Korea Research Institute of Chemical Technology, Taejon, Korea, performed elemental analyses. The free ligand, **L**, was synthesized by a previously reported method. [15]

Caution! The perchlorate salts used in this study are potentially explosive and should be handled in small quantities.

2.2. Syntheses

2.2.1. Synthesis of [Cu(L1)]·(ClO₄)₂ (1)

Methanol (200 mL) solution of **L** (5 g, 1.49 mmol) and $Cu(ClO_4)_2 \cdot 6H_2O$ (5.51 g, 1.49 mmol) were heated at reflux for 30 min. The solution was cooled and the solid was filtered, washed with methanol, and finally air-dried. Suitable crystals of **1**(*cis* fused cyclohexane rings, amber cubic) for X-ray diffraction were obtained by recrystallization from DMF/water and subsequent isolation of the amber crystals manually from the deep blue compound under a microscope. Anal. Calcd. for $C_{20}H_{40}N_4O_8Cl_2Cu$ (**1**) : C, 40.07; H, 6.68; N, 9.35. Found C, 40.38; H, 6.94; N, 9.48.

2.2.2. Synthesis of [Cu(L2)(O₂CH)]·ClO₄ (2)

$[Cu(L)] \cdot (ClO_4)_2$ was dissolved in a minimum amount of DMF/H₂O with several drops of triethylamine. After one week, the target complex **2** was separated out as midnight blue crystals (*trans* fused cyclohexane rings, parallelepiped) just before the solution was dried up. Suitable crystals of **2** for X-ray diffraction studies and subsequent spectroscopic measurements were manually collected under a microscope. A rational synthesis of complex **2** was also achieved in a different route by the reaction between $[Cu(L)] \cdot (ClO_4)_2$ (2 g, 3.34 mmol) and potassium formate (0.28 g, 3.34 mmol) in DMF/H₂O. The crystals of **2** were obtained with minor

impurities. The minor impurities were identified as unreacted starting complex **1** and a diaqua copper(II) complex, $[Cu(\mathbf{L2})(H_2O)_2]Cl_2\cdot 2H_2O$ (*trans* fused cyclohexane rings, bluish purple plate), which was identified by a single crystal X-ray diffraction. Anal. Calcd. for $C_{21}H_{43}N_4O_7ClCu$ (**2**) : C, 44.79; H, 7.64; N, 9.95. Found C, 44.82; H, 7.72; N, 9.87.

2.3. X-ray crystallography

A summary of selected crystallographic data for **1** and **2** is given in Table 1.1. X-ray data were collected on a Nonius Kappa CCD diffractometer using graphite monochromated Mo Kα radiation ($\lambda = 0.71073$ Å). A combination of 1° phi and omega (with kappa offsets) scans were used to collect sufficient data. The data frames were integrated and scaled using the Denzo-SMN package.[17] The structures were solved and refined using the SHELXTL\PC V5.1 package.[18] Refinement was by full-matrix least squares on F^2 using all data (negative intensities included). Hydrogen atoms were included in calculated positions except for those involving hydrogen bonding - specifically for the hydrogen atoms of the water molecule and those bonded to the nitrogen atoms, which were refined with isotropic thermal parameters. For **1**, the Cu-containing cation and the anion have crystallographic inversion symmetry and there are two anions for each cation. For **2**, there are two

Table 1.1. Crystal data and structure refinement for $[Cu(L1)] \cdot (ClO_4)_2$ (**1**) and $[Cu(L2)(O_2CH)] \cdot ClO_4$ (**2**).

	1	2
Empirical formula	$C_{20}H_{40}Cl_2CuN_4O_8$	$C_{21}H_{43}ClCuN_4O_7$
Formula weight	599.0	562.58
Temperature	100.0(1)	150(1)
Wavelength	0.71073	0.71073
Crystal system	Monoclinic	Monoclinic
Space group	C2/c	P2(1)/c
a(Å)	19.8962(6)	8.8005(2)
b(Å)	12.5133(4)	18.6671(4)
c(Å)	11.4168(3)	15.4825(3)
$\beta(°)$	114.929(2)	96.7040(10)
$V(Å^3)$	2577.58(13)	2526.07(9)
Z	2	4
$D_{calcd}(Mg/m^3)$	1.544	1.479
Absorption coefficient(mm^{-1})	1.106	1.019
F(000)	1260	1196
Crystal size(mm)	0.27 x 0.24 x 0.24	0.25 x 0.20 x 0.13
θ range for data collection	3.11 to 27.50°	2.77 to 27.49°
Index ranges	$0 \leq h \leq 25$	$0 \leq h \leq 11$
	$0 \leq k \leq 16$	$0 \leq k \leq 24$
	$-14 \leq l \leq 13$	$-20 \leq l \leq 19$
Reflections collected	14282	28683
Independent reflections	2958 [R(int) = 0.045]	5792 [R(int) = 0.071]
Completeness to θ	99.8 %(θ = 27.50°)	99.8 % (θ= 27.49°)
Absorption correction	multi-scan (Denzo-SMN)	
Max. and min. transmission	0.7771 and 0.7544	0.8790 and 0.7848
Refinement method	Full-matrix least-squares on F^2	
Data/restraints/parameters	2958/0/162	5792/0/346
Goodness-of-fit on F^2	0.975	0.987

Final R indices[I>2σ(I)]	R1=0.0331, wR2=0.0810	R1=0.0357, wR2=0.0813
R indices (all data)	R1=0.0513, wR2=0.0860	R1=0.0619, wR2=0.0876
Largest diff. peak and hole	0.481 and -0.464 e. Å^{-3}	0.344 and -0.421 e. Å^{-3}

$R1 = \Sigma || F_o - F_c || / \Sigma | F_o |$ and $wR2 = [\Sigma [w(F_o^2 - F_c^2)^2] / \Sigma [w(F_o^2)^2]]^{1/2}$.

molecules of crystallized water, which are involved in hydrogen bonding for every cation molecule. The complex had one disordered perchlorate anion (disorder is rotational about the Cl(1)-O(3) bond; 61.8% for O(4), O(5), and O(6) and 38.2% for O(4*), O(5*), O(6*)) and a formate anion.

3. Results and Discussion

3.1. Structures of 1

The structure of **1** confirms the analytical composition and shows that two perchlorate oxygen atoms are axially disposed with respect to the central copper(II) ion (Figure 1.1). The ligand skeleton of the present complex adopts the classical *trans III*(R,R,S,S) conformation with two chair-form six-membered and two gauche five-membered chelate rings. [19, 20] In **1**, both of the ethylene bridges in the macrocycle have been replaced by *cis*-cyclohexane. The interatomic distances (Table 1.2) within the coordination sphere reflect the axially-elongated, octahedrally-coordinated copper(II) ion, with the four equatorially-positioned macrocycle nitrogens each being strongly bonded at 2.0018(15) Å – 2.0453(15) Å, in an essentially square arrangement. These are as expected for this type of macrocyclic ligand complex. [13,14,21,22] In contrast to **2**, compound **1** exhibits a

tetragonally distorted octahedral complex, with two perchlorate anions, each coordinated to the copper atom through one oxygen atom. The axial Cu-O distances of 2.7418(13) Å are among the longest found in related complexes ([Cu(**L4**)]·(ClO$_4$)$_2$; 2.697(5) Å: **L4** = γ-C-*meso*-5,5,7,12,14,14-hexamethyl-1,4,8,11-tetraazacyclotetradecane; and [Cu(**L3**)]·(ClO$_4$)$_2$; 2.57(4) Å), [21,22] probably as a result of the increased steric interactions with the two cyclohexane rings and methyl groups. The long contacts between Cu and O (perchlorate) are also indicative for an elongated Jahn-Teller axis along the O-Cu-O direction, in which the two oxygen atoms are mutually *trans* to each other. In addition to weak Cu-O bonds, two other oxygen atoms of the perchlorate groups are linked to the rest of the molecule by weak intramolecular N-H···O hydrogen bonds, while the fourth O atom remains uninvolved in interactions with the pre-organized macrocycle (Table 1.3). The long Cu-O contact is stabilized by these hydrogen bonding interactions. The Cu-O linkages are bent slightly off the perpendicular to the Cu-N4 plane by 4-5° (Table 1.2). The octahedral amber complex, **1**, is stable in the solid state for a period of several weeks.
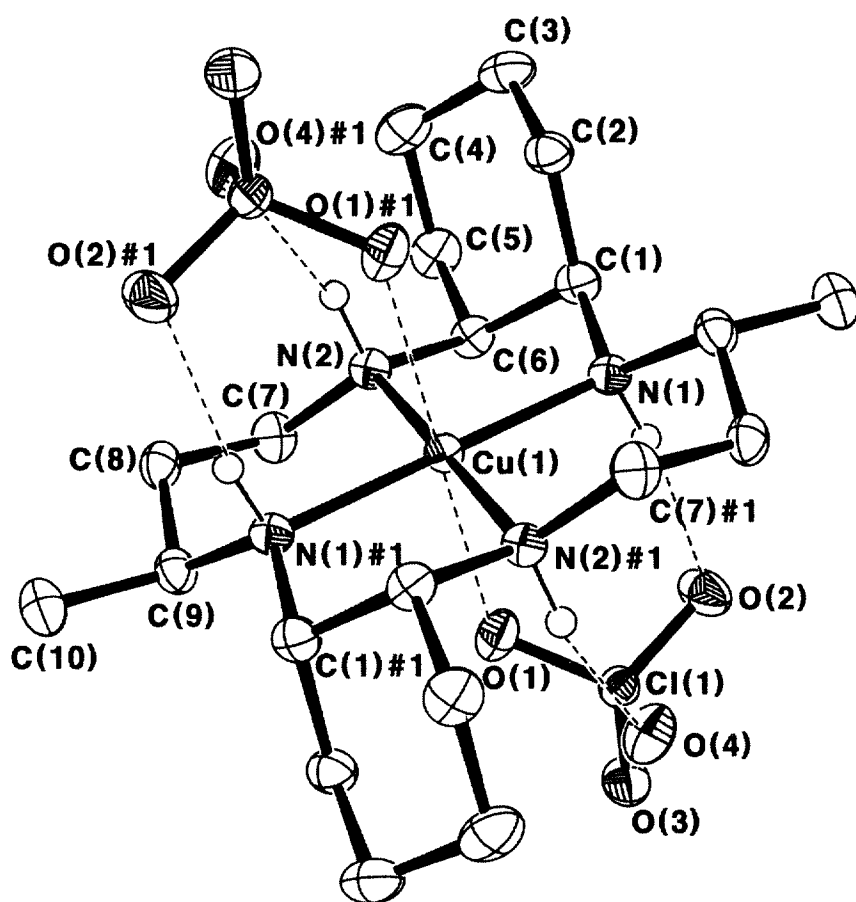
Figure 1.1. Molecular structure of [Cu(**L1**)] · (ClO$_4$)$_2$ (**1**) with atom-labeling scheme. Hydrogen atoms other than those participating in hydrogen bonding are omitted for clarity.

Table 1.2. Selected interatomic distances (Å) and angles (°) for [Cu(**L1**)]·(ClO$_4$)$_2$ (**1**).

Cu(1)-N(1)	2.0453(15)	Cu(1)-N(2)	2.0018(15)
Cu(1)-O(1)	2.0453(15)		
N(2)-Cu(1)-N(2)#1	180.00(9)	N(2)-Cu(1)-N(1)	85.22(6)
N(2)#1-Cu(1)-N(1)	94.78(6)	N(2)-Cu(1)-N(1)#1	94.78(6)
N(2)#1-Cu(1)-N(1)#1	85.22(6)	N(1)-Cu(1)-N(1)#1	180.00(11)
N(2)-Cu(1)-O(1)	84.91(5)	N(2)#1-Cu(1)-O(1)	95.09(5)
N(1)-Cu(1)-O(1)	85.78(5)	N(1)#1-Cu(1)-O(1)	94.22(5)

Symmetry transformations used to generate equivalent atoms:

#1 –x+1/2,-y+1/2,-z

Table 1.3. Hydrogen bonds for [Cu(**L1**)]·(ClO$_4$)$_2$ (**1**) [Å and °].*

D-H...A	d(D-H)	d(H...A)	d(D...A)	<(DHA)
N(1)-H(1)...O(2)	0.93	2.09	3.018(2)	171.8
N(2)-H(2)...O(4)#1	0.93	2.27	3.127(2)	152.2

Symmetry transformations used to generate equivalent atoms:
#1 -x+1/2,-y+1/2,-z

* The hydrogen atoms represented here were all refined isotropically.

3.2. Structures of 2

In **2**, the copper atom is five-coordinate with bonds to the four secondary amine

nitrogen atoms of the macrocyclic ligand and to the oxygen atom of the formate

ligand. The basic ligand geometry in **2** is similar to **1** except for the two cyclohexane

rings which are fused to the central macrocycle as a *trans* fashion. Figure 1.2 shows

the structure of **2** as determined by single crystal X-ray diffraction. A listing of

selected interatomic distances and angles is given in Table 1.4. The ligand skeleton

found in **2** is basically similar to that observed from **1**. The Cu-N atom distances

vary from 2.0216(16) Å to 2.0517(17) Å with an average distance of 2.035 Å. The

Cu-O(formate) distance of 2.2343(15) Å is ~ 15 % longer than the other Cu-O bonds.

The average Cu-O distance of 1.966 ± 0.030 Å, determined from five structures, is

found in a previous report. [23] The uncoordinated oxygen atom of the formate ligand

is hydrogen bonded to one of the hydrogen atoms of the secondary amine N(3) and

the water molecule O(1W). The hydrogen atom attached to N(2) also is hydrogen

bonded to the other water molecule O(1W)#1. The disordered perchlorate anion is

well-separated from the copper atom and the shortest distance between a copper

atom and an oxygen atom of the perchlorate anion is 3.313(4) Å, which is well

outside any previously reported interactions. The remaining two oxygen atoms of

the perchlorate anion are involved in hydrogen bonds with the nitrogen-bound

hydrogen atoms of the secondary amines (Table 1.5).

The pertinent feature of this compound is its coordination geometry around the central copper(II) ion, which is a square pyramid with a tetraazamacrocycle **L2**. Five-coordinated copper(II) complexes are commonly observed in other macrocyclic systems.[24-27] Contrary, most of the previous copper(II) complexes based on ligand **L3** or its derivatives are axially elongated octahedra or square planar around the central metal ion.[13, 14, 28] This trend was observed even with the employment of common axial ligands such as N_3^-, NCS^-, and NCO^- with precursor complex **1**. However, the copper(II) ion in **2** has a preference for adopting a five-coordinate square pyramid where interacting with a formate ligand. The incoming formate ligand displaces only one ClO_4^- anion from **1**. The deviation from the N4 plane to the Cu atom toward the site of the strong fifth coordination location is 0.1269(7) Å as expected. The aforementioned multiple hydrogen bonding interactions along with the high basicity of the formate ligand are believed to stabilize this five-coordinate geometry around the copper(II) ion. The formate ligand coordinates to the copper(II) ion with one oxygen atom, thereby forming a six-membered ring, composed of the copper(II) ion, the three atoms of the formate ligand, the hydrogen atom attached to N(3), and N(3). One of the lattice water molecules also contributes to stabilize the formate ligand through hydrogen bonding. Although the perchlorate anion is far from the copper(II) coordination sphere, the atoms of the perchlorate anion reside in

a location to inhibit further attack of an additional incoming formate ligand. This anion is anchored in place against the back face of the molecule with additional hydrogen bonding interactions. These are present between O(3)#2 and H(2W), H(1) and O(6), and H(4) and O(4*) (Table 1.5).
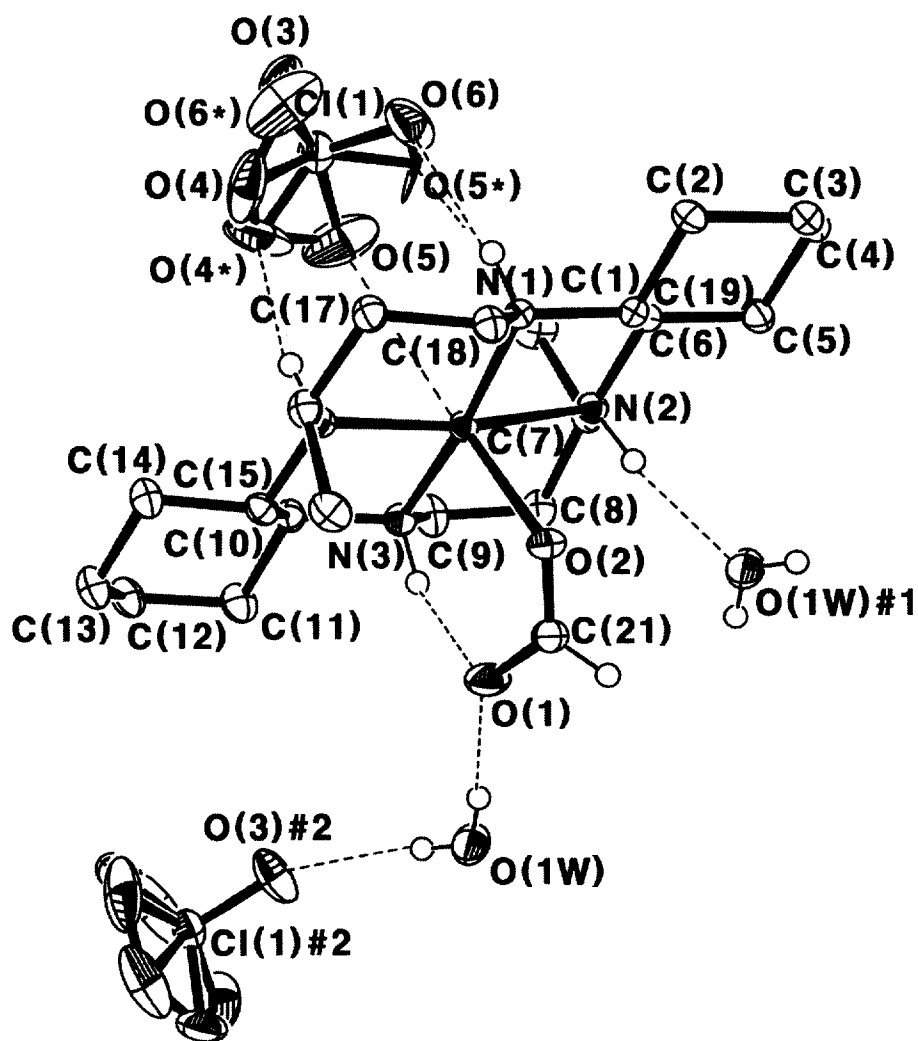
Figure 1.2. Molecular structure of [Cu(**L2**)(O$_2$CH)]·ClO$_4$ (**2**) with atom-labeling scheme. Hydrogen atoms other than those participating in hydrogen bonding are omitted for clarity. The positions of both refined partly occupying are described for the disordered ClO$_4^-$.

Table 1.4. Selected interatomic distances (Å) and angles (°) for [Cu(**L2**)(O₂CH)] · ClO₄ (**2**).

Cu(1)-N(1)	2.0324(16)	Cu(1)-N(2)	2.0347(17)
Cu(1)-N(3)	2.0216(16)	Cu(1)-N(4)	2.0517(17)
Cu(1)-O(2)	2.2343(15)	Cu(1)-O(5)	3.313(4)
O(1)-C(21)	1.243(3)	O(2)-C(21)	1.255(2)
N(3)-Cu(1)-N(1)	172.58(7)	N(3)-Cu(1)-N(2)	96.00(7)
N(1)-Cu(1)-N(2)	85.10(7)	N(3)-Cu(1)-N(4)	84.65(7)
N(1)-Cu(1)-N(4)	92.91(6)	N(2)-Cu(1)-N(4)	169.24(7)
N(3)-Cu(1)-O(2)	98.05(6)	N(1)-Cu(1)-O(2)	89.31(6)
N(2)-Cu(1)-O(2)	87.91(6)	N(4)-Cu(1)-O(2)	102.66(6)
N(3)-Cu(1)-O(5)	90.18(9)	N(1)-Cu(1)-O(5)	82.41(9)
N(2)-Cu(1)-O(5)	97.06(12)	N(4)-Cu(1)-O(5)	72.18(12)
O(2)-Cu(1)-O(5)	169.92(7)	C(21)-O(2)-Cu(1)	122.87(14)
O(1)-C(21)-O(2)	126.6(2)		

Symmetry transformations used to generate equivalent atoms:

Table 1.5. Hydrogen bonds for [Cu(**L2**)(O₂CH)] · ClO₄ (**2**) [Å and °].*

D-H...A	d(D-H)	d(H...A)	d(D...A)	<(DHA)
N(1)-H(1)...O(6)	0.93	2.19	3.113(6)	172.0
N(1)-H(1)...O(5*)	0.93	2.21	3.063(8)	152.6
N(2)-H(2)...O(1W)#1	0.93	2.08	2.974(3)	161.0
N(3)-H(3)...O(1)	0.93	1.99	2.848(2)	152.7
N(4)-H(4)...O(4*)	0.93	2.11	3.021(6)	165.9
O(1W)-H(1W)...O(1)	0.75(3)	1.98(3)	2.727(3)	173(3)
O(1W)-H(2W)...O(3)#2	0.72(3)	2.30(3)	3.013(3)	175(3)

Symmetry transformations used to generate equivalent atoms:

#1 -x+1,-y+1,-z+1   #2 x+1,-y+3/2,z+1/2

* The hydrogen atoms represented here were all refined isotropically.

3.3. Spectroscopy

The solid state infrared spectrum of **1** indicates the presence of coordinated ClO_4^-. Thus, the Cl-O stretching and bending modes are split into two strong absorptions at 1145, 1090, and 627 cm^{-1}, respectively, due to the lowering of the symmetry of the perchlorate ion. Two vN-H bands are observed at 3245 and 3201 cm^{-1}, indicating the presence of the hydrogen bonding arrangement that supports the overall structure in **1**.[29] The spectrum of **2** contains typical uncoordinated vClO_4^- bands at 1121 and 637 cm^{-1}, a vN-H band at 3130 cm^{-1}, and a vCOO$^-$ band at 1633 cm^{-1}, supporting the crystal structure clearly. The strong bands at 1121 and 637 cm^{-1}, originating from Cl-O stretching and bending vibrations, respectively, are not split, which indicates the presence of uncoordinated ClO_4^- anions. [22] A broad band at 3405 cm^{-1} is assigned to vO-H stretching due to the lattice water.

In summary, both ClO_4^- counter anions in **1** are held by pre-organized interactions with the macrocyclic ligand, resulting in Cu-O distances of 2.7418(13) Å. Conversely, for compound **2**, an unusual five-coordinate geometry has been found around the central atom. The apical formate ligand is held in place by hydrogen bonds to the macrocyclic ligand. The sixth coordination site has a perchlorate anion, which interacts with the N4 macrocycle by way of two N-H⋯O hydrogen bonds; however, it does not evidence interaction with the copper center (3.313(4) Å).

Spectroscopic data are consistent with the observed structure of an axially elongated

octahedron for **1**, and an unusual square-based pyramid for **2**.
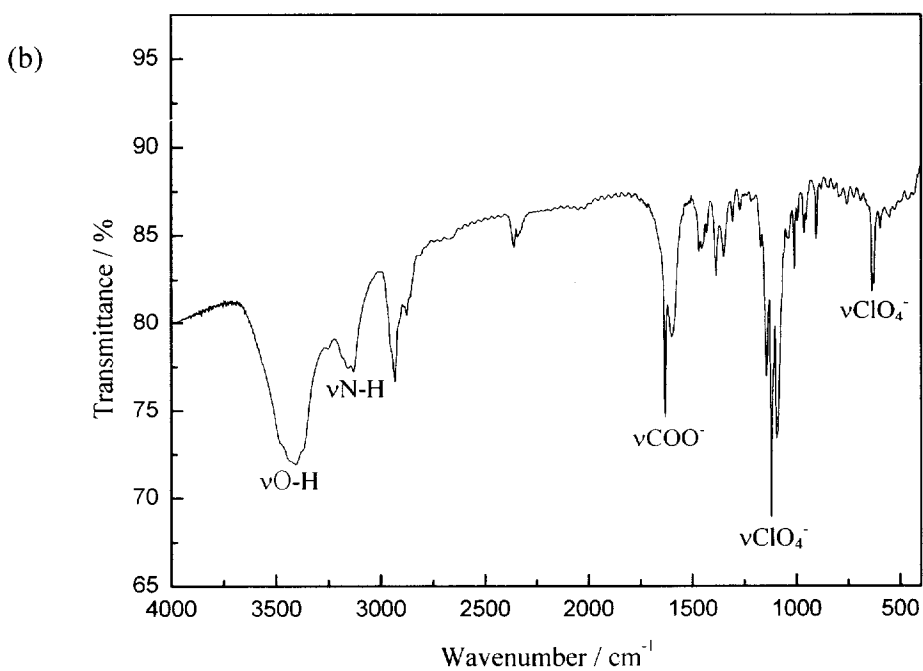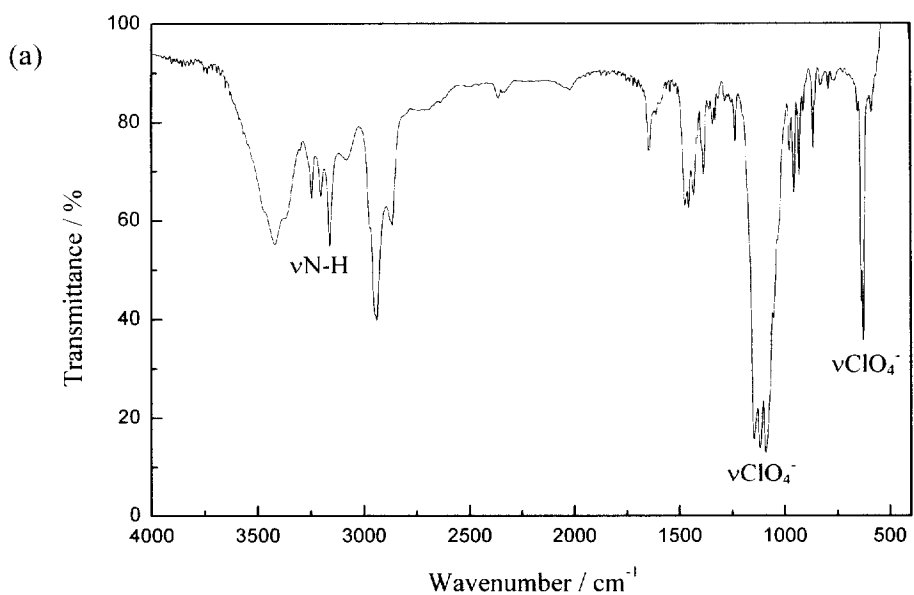
Figure 1.3. Infrared spectra of (a) [Cu(**L1**)]·(ClO$_4$)$_2$ (**1**) and (b) [Cu(**L2**)(O$_2$CH)]·ClO$_4$ (**2**) [KBr pellet]
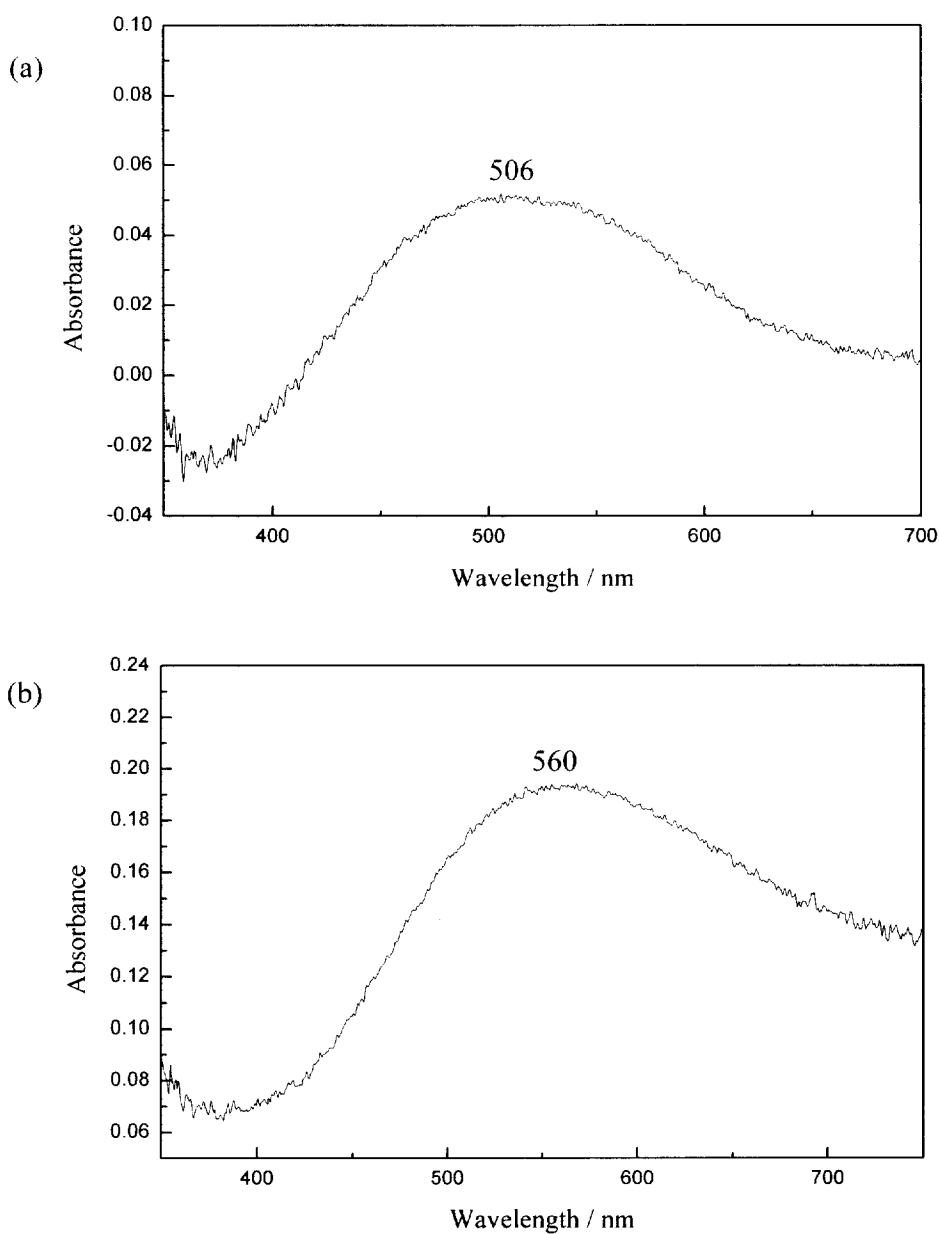
Figure 1.4. Solid state electronic absorption spectra of [Cu(**L1**)]·(ClO$_4$)$_2$ (**1**) and (b) [Cu(**L2**)(O$_2$CH)]·ClO$_4$ (**2**) in BaSO$_4$ by diffuse reflectance method at room temperature.

4. References

[1]   Donnelly, M. A.; Zimmer, M.; *Inorg. Chem.* **1999**, *38*, 1650.

[2]   Daugherty, P. A.; Glerup, J.; Goodson, P. A.; Hodgson, D. J.; Michelson, K.; *Acta Chem. Scand.* **1991**, *45*, 244.

[3]   Sosa, M. E.; Tobe, M. L.; *J. Chem. Soc., Dalton Trans.* **1986**, 427.

[4]   Addison, A. W.; Sinn, E.; *Inorg. Chem.* **1983**, *22*, 1225.

[5]   Amundsen, A. R.; Whelan, J.; Bosnich, B.; *J. Am. Chem. Soc.* **1977**, *99*, 6730.

[6]   Létumier, F.; Broeker, G.; Barbe, J. -M.; Guilard, R.; Lucas, D.; Dahaouï-Gindrey, V.; Lecomte, C.; Thouin, L.; Amatore, C.; *J. Chem. Soc., Dalton Trans.* **1998**, 2233.

[7]   Alcock, N. W.; Berry, A.; Moore, P.; *Acta Crystallogr.,* **1992**, *Sect. C48*, 16.

[8]   Brewer, K. J.; Calvin, M.; Lumpkin, R. S.; Otvos, J. W.; Spreer, L. O.; *Inorg. Chem.* **1989**, *28*, 4446.

[9]   Chan, P. K.; Poon, C. K.; *J. Chem. Soc., Dalton Trans.* **1976**, 858.

[10]   Kang, S. -G.; Kim, M. -S.; Choi, J. -S.; Whang, D.; Kim, K.; *J. Chem. Soc., Dalton Trans.* **1995**, 363.

[11]   Lindoy, L. F. *The Chemistry of Macrocyclic Ligand Complexes*; Cambridge University Press: Cambridge, 1989; pp 14-16.

[12]   Kim, J. C.; Lough, A. J.; *Bull. Korean Chem. Soc.* **1999**, *20*, 1241.

[13]   Kim, J. C.; Fettinger, J. C.; Kim, Y. I.; *Inorg. Chim. Acta* **1999**, *286*, 67.

[14]   Choi, K. -Y.; Kim, J. C.; Jensen, W. P.; Suh, I. -H.; Choi, S. -S.; *Acta Crystallogr.,* **1996**, *Sect. C52*, 2166.

[15]   Kang, S. -G.; Kweon, J. K.; Jung, S. -K.; *Bull. Korean Chem. Soc.* **1991**, *12*,

483.

[16] Choi, K. -Y.; Suh, I. -H.; Kim, J. C.; *Polyhedron* **1997**, *16*, 1783.

[17] Otwinnowski, Z.; Minor, W.; *Methods in Enzymology* **1997**, *276*, 1783.

[18] Sheldrick, G. M.; *SHELXTL\PC V5.1*, Bruker Analytical X-ray Systems: Madison, Wisconsin, U.S.A., 1997.

[19] Adam, K. R.; Antolovich, M.; Brigden, L. G.; Leong, A. J.; Lindoy, L. F.; Baillie, P. J.; Uppall, D. K.; McPartlin, M.; Shah, B.; Proserpio, D.; Fabbrizzi, L.; Tasker, P. A.; *J. Chem. Soc., Dalton Trans.* **1991**, 2493.

[20] Adam, K. R.; Atkinson, I. M.; Lindoy, L. F.; *Inorg. Chem.* **1997**, *36*, 480.

[21] Ochiai, E. -I.; Rettig, S. J.; Trotter, J.; *Can. J. Chem.* **1978**, *56*, 267.

[22] Tasker, P. A.; Sklar, L.; *J. Cryst. Mol. Struct.* **1975**, *5*, 329.

[23] Orpen, A. G.; Brammer, L.; Allen, F. H.; Kennard, O.; Watson, D. G.; Taylor, R.; *J. Chem. Soc., Dalton Trans.* **1989**, S1.

[24] Maroney, M. J.; Rose, N. J.; *Inorg. Chem.* **1984**, *23*, 2252.

[25] Pattrick, G.; Ngwenya, M. P.; Dobson, S. M.; Hancock, R. D.; *J. Chem. Soc., Dalton Trans.* **1991**, 1295.

[26] Salhi, C. A.; Yu, Q.; Heeg, M. J.; Villeneuve, N. M.; Juntunen, K. L.; Schroeder, R. R.; Ochrymowycz, L. A.; Rorabacher, D. B.; *Inorg. Chem.* **1995**, *34*, 6053.

[27] Wijetunge, P.; Kulatilleke, C. P.; Dressel, L. T.; Heeg, M. J.; Ochrymowycz, L. A.; Rorabacher, D. B.; *Inorg. Chem.* **2000**, *39*, 2897.

[28] Choi, K. -Y.; Suh, I. -H.; Kim, J. C.; *Bull. Korean Chem. Soc.* **1997**, *18*, 1321.

[29] Taraszewska, J.; Roslonek, G.; Lampeka, Y. D.; Maloshtan, I. M.; *J. Electroanal. Chem.* **1998**, *452*, 49.

CHAPTER II

Arene Hydroxylation by a bis(*μ*-oxo)dinickel(III) complex

Abstract

A bis(*μ*-oxo)dinickel(III) complex with Me$_4$-pyxyl ligand, which shows the first reactivity of arene hydroxylation by a bis(*μ*-oxo)dinickel(III) core, has been successfully generated by treating the corresponding bis(*μ*-hydroxo)dinickel(II) complex with equimolar amount of H$_2$O$_2$ at low temperature. The bis(*μ*-oxo)dinickel(III) complex exhibits a characteristic UV-vis absorption band at 407 nm and a resonance Raman band at 616 cm^{-1} which shifted to 586 cm^{-1} upon ^{18}O-substitution. Kinetic studies and isotope labeling experiments using H$_2^{18}$O$_2$ imply the existence of intermediate(s) such as peroxo dinickel(II) in the formation process of the bis(*μ*-oxo)dinickel(III) complex. The bis(*μ*-oxo)dinickel(III) complex gradually decomposes, leading to arene hydroxylation of the supporting ligand. Isotope labeling experiment indicates the oxygen source of the phenoxo group is H$_2$O$_2$, which shows the arene hydroxylation involves oxygen transfer from the bis(*μ*-oxo)dinickel(III) core. A similar arene hydroxylation occurred in the Cu system

where (μ-η^2:η^2-peroxo)dicopper(II) complex with the same ligand was observed as an intermediate. Comparison of the structure and reactivity of the active oxygen complexes between the Ni and the Cu systems are discussed.

1. Introduction

Arene hydroxylation by transition metal complexes is of great importance for understanding the reaction mechanism of tyrosinase (Scheme 1).[1] Since the pioneering studies on aromatic ligand hydroxylation by Karlin et. al., (μ-η^2:η^2-peroxo)dicopper(II) intermediates have been regarded as a key step for arene hydroxylation reaction initiated by an electrophilic attack on the aromatic ring.[2] However, Tolman et al. have recently reported an example for arene hydroxylation by bis(μ-oxo)dicopper(III) species.[3] Very recently, a bis(μ-oxo)dicopper(III) complex with a phenolate has also been reported which exhibits hydroxylation of the arene ring through an electrophilic aromatic substitution reaction.[4]
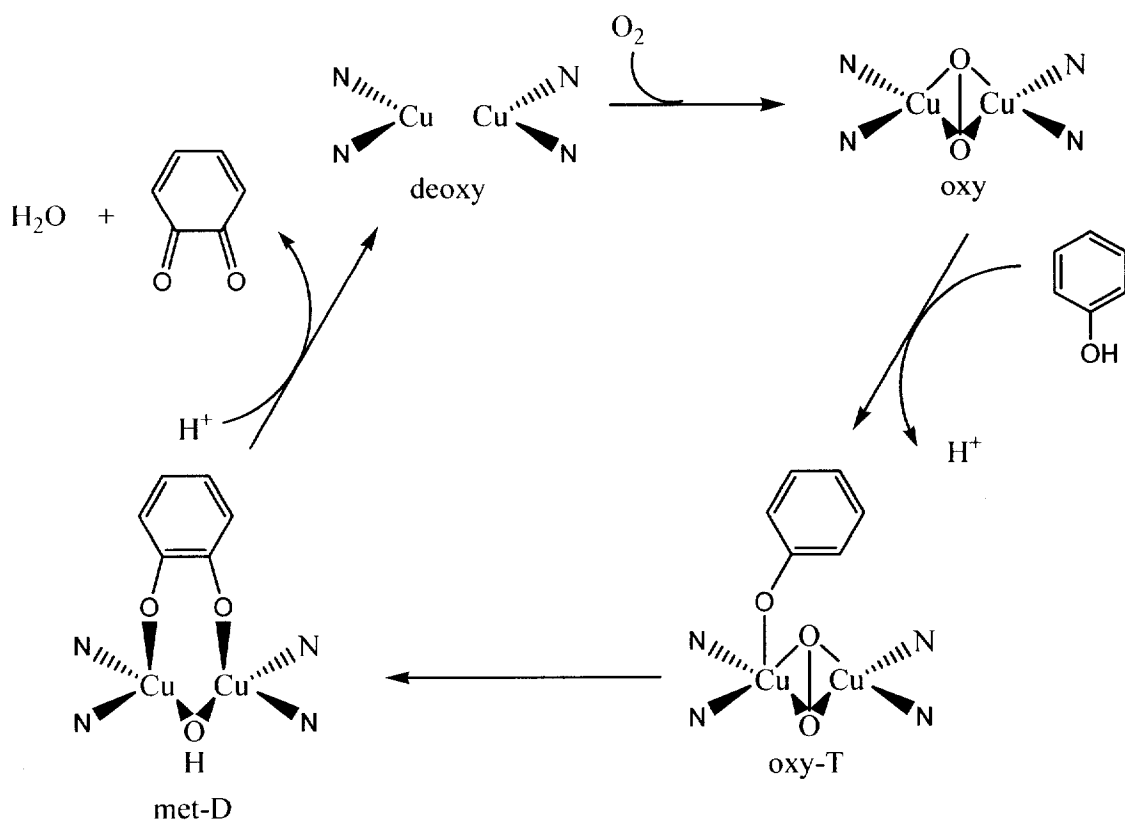
Scheme 1. The reaction mechanism of tyrosinase.

In Cu/O$_2$ chemistry, structural isomers (μ-η^2:η^2-peroxo) and bis(μ-oxo) have been found to be in a rapid equilibrium,[5] which provokes the question of which one is a real active species. To elucidate this dilemma, we have introduced Ni system because theorists suggested that the equilibrium between the (μ-η^2:η^2-peroxo)dinickel(II) and bis(μ-oxo)dinickel(III) core structures is strongly shifted toward the bis(μ-oxo) core in Ni system (Scheme 2).[6] Although arene hydroxylation in the presence of Ni has been reported by Kimura et al., the active oxygen intermediate has not been identified yet.[7] So far, a few bis(μ-oxo)dinickel(III) complexes have been identified, but all of them show reactivity for only aliphatic C-H bond activation.[8]

bis(μ-oxo)   (μ-η^2:η^2-peroxo)
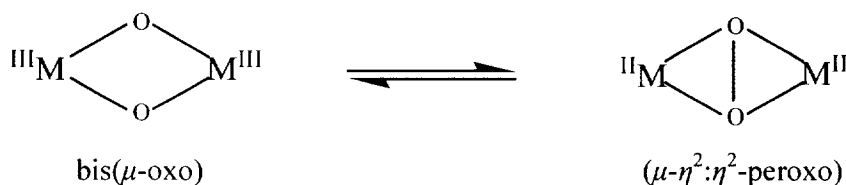
Scheme 2.

Herein, we report on the first arene hydroxylation by a bis(μ-oxo)dinickel(III) complex having Me$_4$-pyxyl ligand. We have very recently reported the same type of arene hydroxylation in the reaction of the Cu(I) complex with O$_2$, where a (μ-η^2:η^2-peroxo)dicopper(II) complex having Me$_4$-pyxyl ligand was observed as a reaction intermediate.[9] Thus, this study provides important insights into the mechanism of arene hydroxylation by comparing two systems based on bis(μ-oxo)dinickel(III) and (μ-η^2:η^2-peroxo)dicopper(II) complexes with the same ligand.

Me$_4$-pyxyl
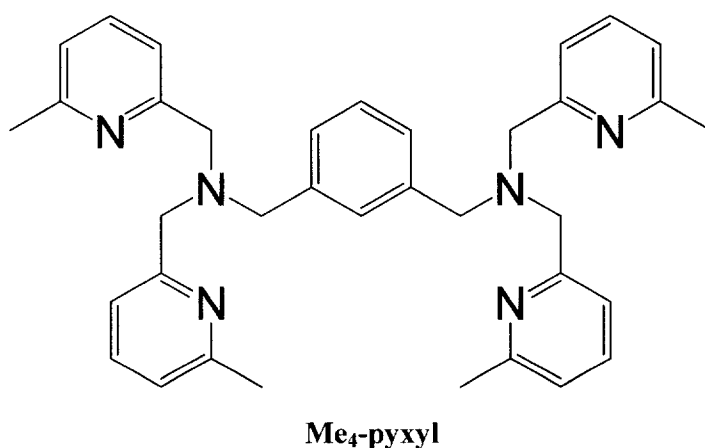
2. Experimental

2.1 Physical measurements

Acetonitrile and acetone were dried over molecular sieves 5 Å and distilled under N_2 atmosphere before use.

UV-vis spectra were measured with a Simadzu diode array spectrometer Multispec-1500 or an Otsuka Electronics photodiode array spectrometer MCPD-2000 with an Otsuka Electronics optical fiber attachment. The temperatures were controlled with a Unisoku thermostated cell holder for the former instrument and with an EYELA low temperature pair stirrer PSL-1800 for the latter one.

Resonance Raman spectra were obtained with a liquid N_2 cooled CCD detector (model LN/CCD-1340 × 400PB, Princeton Instruments) attached to a 1 m-single polychromator (model MC-100dg, Ritsu Oyo Kogaku). The 406.7 nm line of a Kr^+ laser (model 2060 Spectra Physics) was used as an exciting source. The laser powers used were *ca.* 10 mW at the sample point. All measurements were carried out with a spinning cell (1000 rpm) at *ca.* -45 to *ca.* -80 ℃. Raman shifts were calibrated with indene, and the accuracy of the peak positions of the Raman bands was ± 1 cm^{-1}.

ESI-TOF/MS spectra were measured with a Micromass LCT spectrometer. Accurate masses (in *m/z*) are referenced to tetrabutylammonium ion (*m/z* = 242.2848) as an internal standards. ^{1}H-NMR spectra were measured with JEOL

JNM-LM300 or JNM-LM400 using sodium 2,2-dimethyl-2-silapentane-5-sulfonate

(NaDSS) as an internal standard.

2.2. X-ray crystallography

Data collections were carried out on a Rigaku/MSC Mercury diffractometer with

graphite monochromated Mo Kα radiation (λ = 0.71070 Å). The data were collected

at -150 ± 1 ℃.

The structure was solved by a direct method (SIR92)[10] and expanded using a

Fourier technique.[11] The structure was refined by a full-matrix least-squares

method by using the teXan[12] crystallographic software package (Molecular

Structure Corporation). The structure refinement was carried out by the observations

($I > 3.0\sigma(I)$). Non-hydrogen atoms, except for those of solvent molecules, were

refined with anisotropic displacement parameters. Hydrogen atoms were positioned

at calculated positions (0.95 Å). They were included, but not refined, in the final

least-squares cycles.

2.3 synthesis and characterization of [Ni$_2$(O)$_2$(Me$_4$-pyxyl)]$^{2+}$ (2)

A bis(μ-hydroxo)dinickel(II) complex, [Ni$_2$(OH)$_2$(Me$_4$-pyxyl)]$^{2+}$ (**1**), has been prepared as a precursor complex by addition of triethylamine to the ethanol solution (20 ml) of Ni(ClO$_4$)$_2$·6H$_2$O (183 mg, 0.5 mmol) and Me$_4$-pyxyl (139 mg, 0.25 mmol). Molecular structure for a bis(μ-methoxo)dinickel(II) complex is given in Figure 2.1. The reaction of **1** in acetone with 1 equiv. of H$_2$O$_2$ at −75°C leads to a spectral change from light blue to dark brown, where a characteristic absorption band at 407 nm ($\varepsilon = 4700$ M^{-1} cm^{-1}) has gradually developed due to the generation of an intermediate species (Figure 2.2). Titration of **1** with H$_2$O$_2$ at 407 nm indicates that the stoichiometry of the reaction between **1** and H$_2$O$_2$ is 1:1 (Figure 2.3). Moreover, a resonance Raman spectrum of the intermediate exhibits an isotope-sensitive band at 616 cm^{-1} that shifts to 586 cm^{-1} for an ^{18}O-labeled sample prepared by H$_2$^{18}O$_2$ (Figure 2.4).
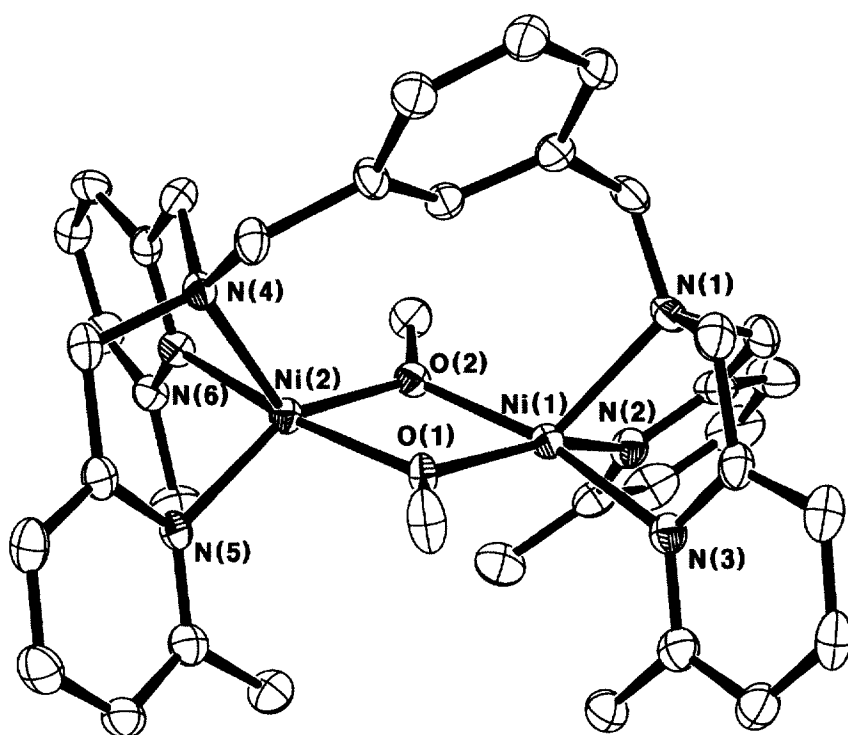
Figure 2.1. Molecular structure of [Ni$_2$(OCH$_3$)$_2$(Me$_4$-pyxyl)] (**1b**) with atom-labeling scheme. Hydrogen atoms are omitted for clarity.

Table 2.1. Atomic coordinates and B_{eq} for [Ni$_2$(OCH$_3$)$_2$(Me$_4$-pyxyl)]

atom	x	y	Z	B_{eq}
Ni(1)	0.47530(6)	0.75394(3)	0.81577(3)	0.0169(1)
Ni(2)	0.41457(6)	0.76943(3)	0.68374(3)	0.0171(1)
Ni(3)	0.18602(6)	0.27878(3)	0.69370(2)	0.0161(1)
Ni(4)	0.08423(6)	0.27166(3)	0.82542(2)	0.0160(1)
Cl(1)	0.8018(3)	0.0554(2)	0.5004(1)	0.0319(6)
Cl(2)	-0.2124(1)	0.01854(8)	0.76291(8)	0.0374(4)
Cl(3)	0.2294(2)	-0.0013(1)	0.99994(10)	0.0222(5)
Cl(4)	0.2549(1)	0.50135(7)	0.97120(5)	0.0206(2)
Cl(5)	-0.2441(1)	0.46528(7)	0.50463(5)	0.0246(3)
O(1)	0.5652(3)	0.7624(2)	0.7372(1)	0.0197(7)
O(2)	0.3296(3)	0.7570(2)	0.7622(1)	0.0178(7)
O(3)	0.2478(3)	0.2768(2)	0.7712(1)	0.0192(7)
O(4)	0.0188(3)	0.2775(2)	0.7473(1)	0.0175(7)
O(5)	0.7585(10)	0.1347(5)	0.4862(4)	0.038(2)
O(6)	0.948(1)	0.0232(8)	0.4771(5)	0.069(4)
O(7)	0.748(1)	0.0166(5)	0.4734(3)	0.051(3)
O(8)	0.792(1)	0.0389(6)	0.5605(4)	0.046(3)
O(9)	-0.1536(6)	0.0681(3)	0.7266(3)	0.059(2)
O(10)	-0.2566(6)	-0.0266(3)	0.7281(3)	0.057(2)
O(11)	-0.1073(5)	-0.0321(3)	0.7991(3)	0.062(2)
O(12)	-0.3296(6)	0.0639(3)	0.7969(3)	0.061(2)
O(13)	0.1275(8)	0.0406(4)	0.9672(3)	0.030(2)
O(14)	0.3401(9)	-0.0397(6)	0.9619(4)	0.045(3)
O(15)	0.173(2)	-0.0521(7)	1.0330(4)	0.079(4)
O(16)	0.278(1)	0.0388(8)	1.0362(5)	0.070(4)
O(17)	0.3468(4)	0.4437(2)	0.9354(2)	0.037(1)
O(18)	0.1632(4)	0.4699(3)	1.0082(2)	0.037(1)
O(19)	0.3362(4)	0.5279(3)	1.0060(2)	0.035(1)
O(20)	0.1719(4)	0.5650(2)	0.9343(2)	0.038(1)
O(21)	-0.1100(4)	0.4403(2)	0.4713(2)	0.0337(10)

O(22)	-0.2880(6)	0.5478(2)	0.5086(2)	0.046(1)
O(23)	-0.3442(5)	0.4474(4)	0.4748(2)	0.058(2)
O(24)	-0.2323(5)	0.4277(3)	0.5623(2)	0.035(1)
N(1)	0.5210(4)	0.6480(2)	0.8685(2)	0.0189(9)
N(2)	0.3266(4)	0.7956(2)	0.8817(2)	0.0179(9)
N(3)	0.6505(4)	0.7522(2)	0.8558(2)	0.0182(9)
N(4)	0.4790(4)	0.6771(2)	0.6293(2)	0.0207(9)
N(5)	0.5034(4)	0.8216(2)	0.6158(2)	0.0226(10)
N(6)	0.2273(4)	0.7858(2)	0.6461(2)	0.0200(9)
N(7)	0.1257(4)	0.3789(2)	0.6367(2)	0.0162(8)
N(8)	0.3804(4)	0.2719(2)	0.6497(2)	0.0194(9)
N(9)	0.1210(4)	0.2313(2)	0.6315(2)	0.0180(9)
N(10)	0.0227(4)	0.3690(2)	0.8753(2)	0.0167(8)
N(11)	0.2106(4)	0.2203(2)	0.8919(2)	0.0189(9)
N(12)	-0.1058(4)	0.2672(2)	0.8657(2)	0.0171(8)
C(1)	0.5566(5)	0.5909(3)	0.7502(2)	0.022(1)
C(2)	0.5851(5)	0.5613(3)	0.6955(2)	0.022(1)
C(3)	0.5767(6)	0.4886(3)	0.6901(2)	0.025(1)
C(4)	0.5326(6)	0.4491(3)	0.7385(2)	0.026(1)
C(5)	0.4967(6)	0.4807(3)	0.7912(2)	0.026(1)
C(6)	0.5107(5)	0.5528(3)	0.7982(2)	0.021(1)
C(7)	0.6103(6)	0.6111(3)	0.6433(2)	0.025(1)
C(8)	0.4986(6)	0.7122(3)	0.5690(2)	0.026(1)
C(9)	0.5449(5)	0.7806(3)	0.5698(2)	0.026(1)
C(10)	0.6177(7)	0.8037(3)	0.5198(3)	0.037(1)
C(11)	0.6467(7)	0.8706(4)	0.5212(3)	0.042(2)
C(12)	0.6057(6)	0.9131(4)	0.5682(3)	0.038(2)
C(13)	0.5323(5)	0.8874(3)	0.6173(2)	0.026(1)
C(14)	0.4857(7)	0.9330(3)	0.6692(3)	0.034(1)
C(15)	0.3538(6)	0.6524(3)	0.6316(2)	0.027(1)
C(16)	0.2223(6)	0.7205(3)	0.6272(2)	0.023(1)
C(17)	0.1024(6)	0.7160(3)	0.6057(2)	0.028(1)

C(18)	-0.0183(6)	0.7816(4)	0.6065(2)	0.030(1)
C(19)	-0.0142(6)	0.8482(3)	0.6267(2)	0.029(1)
C(20)	0.1112(5)	0.8496(3)	0.6455(2)	0.024(1)
C(21)	0.1255(6)	0.9203(3)	0.6653(2)	0.030(1)
C(22)	0.4657(5)	0.5865(3)	0.8564(2)	0.021(1)
C(23)	0.4630(5)	0.6723(3)	0.9277(2)	0.023(1)
C(24)	0.3292(5)	0.7399(3)	0.9251(2)	0.020(1)
C(25)	0.2170(5)	0.7491(3)	0.9667(2)	0.025(1)
C(26)	0.1040(5)	0.8161(3)	0.9641(2)	0.028(1)
C(27)	0.1047(5)	0.8738(3)	0.9191(2)	0.025(1)
C(28)	0.2172(5)	0.8611(3)	0.8782(2)	0.022(1)
C(29)	0.2177(6)	0.9204(3)	0.8288(2)	0.028(1)
C(30)	0.6759(5)	0.6168(3)	0.8680(2)	0.022(1)
C(31)	0.7343(5)	0.6810(3)	0.8724(2)	0.020(1)
C(32)	0.8681(5)	0.6669(3)	0.8915(2)	0.023(1)
C(33)	0.9174(5)	0.7265(3)	0.8917(2)	0.027(1)
C(34)	0.8313(5)	0.8017(3)	0.8745(2)	0.027(1)
C(35)	0.6950(5)	0.8135(3)	0.8589(2)	0.021(1)
C(36)	0.5938(6)	0.8924(3)	0.8450(3)	0.033(1)
C(37)	0.7068(5)	0.7558(3)	0.7215(2)	0.028(1)
C(38)	0.2019(6)	0.7446(4)	0.7785(2)	0.031(1)
C(39)	0.0177(5)	0.4464(3)	0.7557(2)	0.0192(10)
C(40)	0.0025(5)	0.4847(3)	0.7009(2)	0.0181(10)
C(41)	0.0150(5)	0.5575(3)	0.6920(2)	0.023(1)
C(42)	0.0486(6)	0.5897(3)	0.7375(2)	0.027(1)
C(43)	0.0712(5)	0.5485(3)	0.7923(2)	0.024(1)
C(44)	0.0551(5)	0.4755(3)	0.8022(2)	0.0188(10)
C(45)	-0.0101(5)	0.4445(3)	0.6495(2)	0.021(1)
C(46)	0.1179(5)	0.3525(3)	0.5785(2)	0.021(1)
C(47)	0.0817(5)	0.2791(3)	0.5839(2)	0.020(1)
C(48)	0.0161(5)	0.2612(3)	0.5402(2)	0.025(1)
C(49)	-0.0085(6)	0.1919(3)	0.5457(2)	0.026(1)

C(50)	0.0304(6)	0.1430(3)	0.5947(2)	0.027(1)
C(51)	0.0951(5)	0.1639(3)	0.6379(2)	0.022(1)
C(52)	0.1369(6)	0.1117(3)	0.6930(2)	0.027(1)
C(53)	0.2472(5)	0.4076(2)	0.6338(2)	0.0192(10)
C(54)	0.3809(5)	0.3418(3)	0.6262(2)	0.020(1)
C(55)	0.5003(5)	0.3525(3)	0.5973(2)	0.026(1)
C(56)	0.6243(5)	0.2891(3)	0.5945(3)	0.032(1)
C(57)	0.6226(5)	0.2177(3)	0.6191(3)	0.031(1)
C(58)	0.4975(5)	0.2106(3)	0.6460(2)	0.023(1)
C(59)	0.4894(6)	0.1343(3)	0.6706(3)	0.036(1)
C(60)	0.0831(5)	0.4320(3)	0.8607(2)	0.020(1)
C(61)	0.0627(5)	0.3353(3)	0.9349(2)	0.021(1)
C(62)	0.1967(5)	0.2673(3)	0.9340(2)	0.0190(10)
C(63)	0.2936(6)	0.2513(3)	0.9757(2)	0.029(1)
C(64)	0.4063(6)	0.1830(4)	0.9758(2)	0.033(1)
C(65)	0.4193(5)	0.1340(3)	0.9334(2)	0.029(1)
C(66)	0.3219(5)	0.1539(3)	0.8909(2)	0.023(1)
C(67)	0.3341(5)	0.1028(3)	0.8436(3)	0.029(1)
C(68)	-0.1341(5)	0.4009(3)	0.8757(2)	0.020(1)
C(69)	-0.1937(5)	0.3365(3)	0.8806(2)	0.020(1)
C(70)	-0.3328(5)	0.3476(3)	0.8983(2)	0.021(1)
C(71)	-0.3836(5)	0.2880(3)	0.8988(2)	0.024(1)
C(72)	-0.2947(5)	0.2175(3)	0.8833(2)	0.026(1)
C(73)	-0.1546(5)	0.2077(3)	0.8671(2)	0.022(1)
C(74)	-0.0504(6)	0.1312(3)	0.8517(2)	0.026(1)
C(75)	0.3735(6)	0.2843(4)	0.7850(2)	0.030(1)
C(76)	-0.1182(5)	0.2861(3)	0.7315(2)	0.024(1)

Table 2.2. Anisotropic displacement parameters for [Ni$_2$(OCH$_3$)$_2$(Me$_4$-pyxyl)]

atom	U_{11}	U_{22}	U_{33}	U_{12}	U_{13}	U_{23}
Ni(1)	0.0185(3)	0.0173(3)	0.0162(3)	-0.0075(2)	-0.0017(2)	-0.0009(2)
Ni(2)	0.0201(3)	0.0157(3)	0.0161(3)	-0.0073(2)	-0.0004(2)	-0.0008(2)
Ni(3)	0.0180(3)	0.0159(3)	0.0152(3)	-0.0069(2)	-0.0006(2)	-0.0009(2)
Ni(4)	0.0174(3)	0.0163(3)	0.0151(3)	-0.0069(2)	-0.0001(2)	-0.0008(2)
Cl(1)	0.043(1)	0.028(1)	0.031(1)	-0.020(1)	-0.009(1)	0.0045(10)
Cl(2)	0.0233(6)	0.0349(7)	0.0570(9)	-0.0123(5)	-0.0031(6)	-0.0070(6)
Cl(3)	0.0227(10)	0.026(1)	0.0178(9)	-0.0080(9)	0.0007(8)	-0.0022(8)
Cl(4)	0.0173(5)	0.0265(5)	0.0182(5)	-0.0076(4)	-0.0012(4)	-0.0015(4)
Cl(5)	0.0271(6)	0.0273(5)	0.0181(5)	-0.0067(5)	-0.0015(4)	-0.0033(4)
O(1)	0.019(1)	0.020(1)	0.020(2)	-0.006(1)	0.000(1)	-0.003(1)
O(2)	0.020(1)	0.025(2)	0.012(1)	-0.012(1)	-0.001(1)	-0.003(1)
O(3)	0.019(1)	0.030(2)	0.012(1)	-0.012(1)	0.000(1)	-0.002(1)
O(4)	0.017(1)	0.019(1)	0.018(1)	-0.007(1)	-0.001(1)	-0.003(1)
O(5)	0.046(5)	0.034(4)	0.043(5)	-0.024(4)	-0.017(4)	0.009(4)
O(6)	0.062(7)	0.077(8)	0.060(7)	-0.022(6)	0.017(6)	0.008(6)
O(7)	0.118(9)	0.025(4)	0.023(4)	-0.047(5)	0.033(5)	-0.012(3)
O(8)	0.067(6)	0.047(5)	0.028(4)	-0.025(5)	0.000(4)	-0.006(4)
O(9)	0.051(3)	0.049(3)	0.082(4)	-0.029(2)	0.021(3)	-0.010(3)
O(10)	0.052(3)	0.043(3)	0.086(4)	-0.025(2)	-0.021(3)	-0.008(3)
O(11)	0.038(3)	0.061(3)	0.087(4)	-0.011(2)	-0.034(3)	-0.003(3)
O(12)	0.042(3)	0.053(3)	0.081(4)	-0.012(2)	0.014(3)	-0.011(3)
O(13)	0.025(3)	0.033(4)	0.018(3)	0.011(3)	-0.004(3)	-0.006(3)
O(14)	0.026(4)	0.064(6)	0.039(5)	-0.002(4)	0.001(4)	-0.020(4)
O(15)	0.17(1)	0.067(7)	0.027(5)	-0.083(9)	0.001(7)	0.009(5)
O(16)	0.092(9)	0.100(10)	0.049(6)	-0.067(8)	0.005(6)	-0.031(6)
O(17)	0.032(2)	0.037(2)	0.039(2)	-0.004(2)	0.003(2)	-0.018(2)
O(18)	0.033(2)	0.059(3)	0.027(2)	-0.028(2)	0.004(2)	0.003(2)
O(19)	0.026(2)	0.057(3)	0.030(2)	-0.021(2)	0.000(2)	-0.011(2)
O(20)	0.031(2)	0.035(2)	0.042(2)	-0.005(2)	-0.011(2)	0.011(2)

O(21)	0.034(2)	0.037(2)	0.021(2)	-0.004(2)	0.006(2)	0.005(2)
O(22)	0.072(3)	0.028(2)	0.029(2)	-0.010(2)	0.019(2)	-0.008(2)
O(23)	0.046(3)	0.087(4)	0.053(3)	-0.025(3)	-0.006(2)	-0.040(3)
O(24)	0.039(2)	0.042(2)	0.024(2)	-0.017(2)	0.004(2)	0.003(2)
N(1)	0.020(2)	0.022(2)	0.015(2)	-0.006(1)	0.000(1)	-0.003(1)
N(2)	0.021(2)	0.020(2)	0.016(2)	-0.009(1)	-0.002(1)	-0.005(1)
N(3)	0.017(2)	0.019(2)	0.021(2)	-0.009(1)	0.000(1)	-0.003(1)
N(4)	0.030(2)	0.015(2)	0.016(2)	-0.007(2)	0.002(2)	-0.003(1)
N(5)	0.027(2)	0.023(2)	0.020(2)	-0.010(2)	-0.002(2)	0.002(1)
N(6)	0.024(2)	0.021(2)	0.017(2)	-0.010(2)	-0.001(1)	0.000(1)
N(7)	0.018(2)	0.016(2)	0.015(2)	-0.006(1)	-0.001(1)	0.001(1)
N(8)	0.020(2)	0.020(2)	0.020(2)	-0.010(1)	0.003(1)	-0.004(1)
N(9)	0.020(2)	0.021(2)	0.015(2)	-0.009(1)	0.002(1)	-0.005(1)
N(10)	0.020(2)	0.018(2)	0.014(2)	-0.009(1)	0.000(1)	-0.003(1)
N(11)	0.017(2)	0.021(2)	0.018(2)	-0.006(1)	-0.002(1)	0.002(1)
N(12)	0.021(2)	0.019(2)	0.015(2)	-0.012(1)	-0.001(1)	-0.001(1)
C(1)	0.030(2)	0.015(2)	0.019(2)	-0.006(2)	-0.003(2)	0.002(2)
C(2)	0.026(2)	0.019(2)	0.020(2)	-0.005(2)	-0.002(2)	0.001(2)
C(3)	0.035(3)	0.018(2)	0.020(2)	-0.007(2)	-0.004(2)	-0.002(2)
C(4)	0.037(3)	0.018(2)	0.028(2)	-0.012(2)	-0.010(2)	0.002(2)
C(5)	0.030(2)	0.023(2)	0.026(2)	-0.010(2)	-0.003(2)	-0.002(2)
C(6)	0.028(2)	0.018(2)	0.019(2)	-0.010(2)	-0.003(2)	-0.005(2)
C(7)	0.033(3)	0.021(2)	0.019(2)	-0.006(2)	0.005(2)	-0.007(2)
C(8)	0.036(3)	0.027(2)	0.014(2)	-0.008(2)	0.002(2)	-0.002(2)
C(9)	0.025(2)	0.021(2)	0.025(2)	-0.002(2)	0.003(2)	0.002(2)
C(10)	0.041(3)	0.031(3)	0.031(3)	-0.005(2)	0.012(2)	0.001(2)
C(11)	0.034(3)	0.040(3)	0.046(4)	-0.013(3)	0.008(3)	0.015(3)
C(12)	0.029(3)	0.037(3)	0.051(4)	-0.020(2)	-0.002(2)	0.014(3)
C(13)	0.025(2)	0.021(2)	0.031(3)	-0.010(2)	-0.005(2)	0.007(2)
C(14)	0.041(3)	0.022(2)	0.045(3)	-0.015(2)	-0.001(3)	-0.005(2)
C(15)	0.039(3)	0.021(2)	0.024(2)	-0.015(2)	-0.007(2)	0.000(2)
C(16)	0.033(3)	0.024(2)	0.016(2)	-0.013(2)	-0.005(2)	0.002(2)

C(17)	0.035(3)	0.034(3)	0.021(2)	-0.019(2)	-0.007(2)	0.002(2)
C(18)	0.035(3)	0.044(3)	0.017(2)	-0.020(2)	-0.006(2)	-0.001(2)
C(19)	0.026(2)	0.035(3)	0.023(2)	-0.008(2)	-0.004(2)	0.001(2)
C(20)	0.028(2)	0.025(2)	0.020(2)	-0.010(2)	-0.001(2)	0.002(2)
C(21)	0.038(3)	0.024(2)	0.026(2)	-0.006(2)	-0.004(2)	-0.003(2)
C(22)	0.030(2)	0.023(2)	0.014(2)	-0.013(2)	-0.001(2)	0.001(2)
C(23)	0.030(2)	0.028(2)	0.015(2)	-0.014(2)	0.000(2)	-0.002(2)
C(24)	0.022(2)	0.024(2)	0.019(2)	-0.012(2)	-0.003(2)	-0.005(2)
C(25)	0.026(2)	0.037(3)	0.017(2)	-0.018(2)	0.001(2)	0.002(2)
C(26)	0.024(2)	0.036(3)	0.025(2)	-0.012(2)	0.006(2)	-0.006(2)
C(27)	0.022(2)	0.026(2)	0.028(2)	-0.005(2)	-0.004(2)	-0.008(2)
C(28)	0.026(2)	0.021(2)	0.023(2)	-0.011(2)	-0.002(2)	-0.004(2)
C(29)	0.031(3)	0.024(2)	0.030(3)	-0.011(2)	-0.003(2)	0.001(2)
C(30)	0.023(2)	0.022(2)	0.021(2)	-0.008(2)	-0.006(2)	0.002(2)
C(31)	0.018(2)	0.028(2)	0.015(2)	-0.008(2)	0.000(2)	-0.003(2)
C(32)	0.018(2)	0.024(2)	0.026(2)	-0.002(2)	-0.001(2)	-0.005(2)
C(33)	0.020(2)	0.041(3)	0.022(2)	-0.014(2)	0.000(2)	0.000(2)
C(34)	0.022(2)	0.029(2)	0.032(3)	-0.014(2)	-0.003(2)	0.000(2)
C(35)	0.020(2)	0.021(2)	0.023(2)	-0.009(2)	-0.002(2)	-0.004(2)
C(36)	0.030(3)	0.021(2)	0.050(3)	-0.010(2)	-0.005(2)	-0.003(2)
C(37)	0.024(2)	0.032(3)	0.027(2)	-0.010(2)	0.001(2)	0.000(2)
C(38)	0.032(3)	0.054(3)	0.019(2)	-0.031(3)	0.004(2)	-0.007(2)
C(39)	0.019(2)	0.016(2)	0.021(2)	-0.004(2)	0.003(2)	-0.006(2)
C(40)	0.016(2)	0.017(2)	0.021(2)	-0.004(2)	0.000(2)	-0.005(2)
C(41)	0.028(2)	0.016(2)	0.024(2)	-0.006(2)	-0.003(2)	0.002(2)
C(42)	0.037(3)	0.023(2)	0.026(2)	-0.017(2)	0.003(2)	-0.004(2)
C(43)	0.030(2)	0.019(2)	0.027(2)	-0.014(2)	0.006(2)	-0.007(2)
C(44)	0.021(2)	0.015(2)	0.022(2)	-0.008(2)	0.005(2)	-0.005(2)
C(45)	0.019(2)	0.022(2)	0.022(2)	-0.004(2)	-0.003(2)	-0.004(2)
C(46)	0.025(2)	0.024(2)	0.015(2)	-0.009(2)	0.000(2)	-0.002(2)
C(47)	0.021(2)	0.024(2)	0.017(2)	-0.009(2)	-0.001(2)	-0.003(2)
C(48)	0.029(2)	0.029(2)	0.020(2)	-0.013(2)	-0.004(2)	-0.004(2)

C(49)	0.028(2)	0.030(2)	0.024(2)	-0.015(2)	-0.003(2)	-0.004(2)
C(50)	0.031(3)	0.026(2)	0.027(2)	-0.014(2)	0.002(2)	-0.003(2)
C(51)	0.024(2)	0.022(2)	0.023(2)	-0.009(2)	0.003(2)	-0.006(2)
C(52)	0.033(3)	0.022(2)	0.029(3)	-0.014(2)	-0.004(2)	0.001(2)
C(53)	0.028(2)	0.015(2)	0.015(2)	-0.009(2)	0.001(2)	0.000(1)
C(54)	0.024(2)	0.026(2)	0.016(2)	-0.015(2)	0.001(2)	-0.002(2)
C(55)	0.022(2)	0.025(2)	0.030(2)	-0.009(2)	0.004(2)	0.000(2)
C(56)	0.016(2)	0.035(3)	0.044(3)	-0.011(2)	0.015(2)	-0.005(2)
C(57)	0.018(2)	0.023(2)	0.048(3)	-0.002(2)	0.004(2)	-0.007(2)
C(58)	0.020(2)	0.022(2)	0.025(2)	-0.008(2)	0.002(2)	0.000(2)
C(59)	0.033(3)	0.021(2)	0.048(3)	-0.004(2)	-0.005(2)	0.004(2)
C(60)	0.019(2)	0.020(2)	0.022(2)	-0.006(2)	0.001(2)	-0.005(2)
C(61)	0.025(2)	0.027(2)	0.015(2)	-0.012(2)	-0.001(2)	-0.005(2)
C(62)	0.022(2)	0.023(2)	0.014(2)	-0.012(2)	0.000(2)	0.002(2)
C(63)	0.026(2)	0.043(3)	0.020(2)	-0.015(2)	-0.001(2)	0.000(2)
C(64)	0.027(3)	0.045(3)	0.028(3)	-0.014(2)	-0.008(2)	0.004(2)
C(65)	0.023(2)	0.034(3)	0.026(2)	-0.008(2)	-0.005(2)	0.006(2)
C(66)	0.020(2)	0.021(2)	0.029(2)	-0.010(2)	-0.001(2)	0.008(2)
C(67)	0.020(2)	0.022(2)	0.040(3)	-0.001(2)	-0.004(2)	-0.005(2)
C(68)	0.018(2)	0.022(2)	0.019(2)	-0.005(2)	0.000(2)	-0.001(2)
C(69)	0.020(2)	0.026(2)	0.015(2)	-0.009(2)	-0.001(2)	0.001(2)
C(70)	0.023(2)	0.024(2)	0.015(2)	-0.006(2)	-0.001(2)	0.002(2)
C(71)	0.016(2)	0.038(3)	0.018(2)	-0.011(2)	0.001(2)	0.000(2)
C(72)	0.027(2)	0.027(2)	0.027(2)	-0.014(2)	-0.001(2)	-0.002(2)
C(73)	0.028(2)	0.020(2)	0.022(2)	-0.014(2)	-0.003(2)	0.002(2)
C(74)	0.028(2)	0.022(2)	0.030(3)	-0.013(2)	-0.001(2)	-0.002(2)
C(75)	0.028(2)	0.055(3)	0.017(2)	-0.027(2)	-0.001(2)	-0.001(2)
C(76)	0.020(2)	0.032(2)	0.023(2)	-0.011(2)	-0.004(2)	-0.003(2)

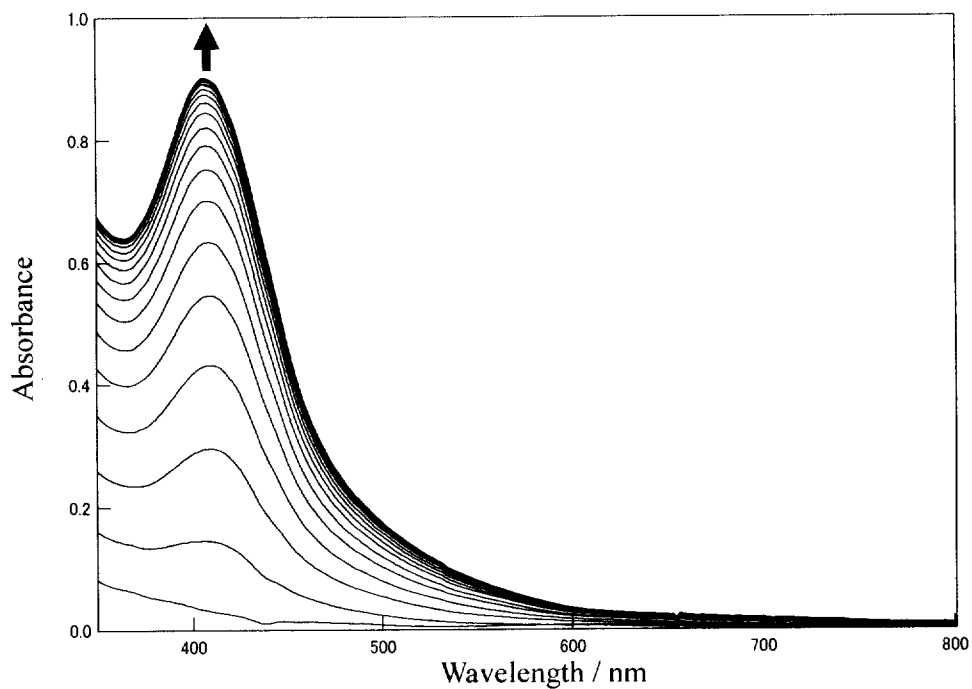**Figure 2.2.** Spectral change in the reaction of $[Ni_2(OH)_2(Me_4\text{-pyxyl})]^{2+}$ **(1)** with 1

equiv. of H_2O_2 in acetone at $-75\ °C$ (4 min interval).
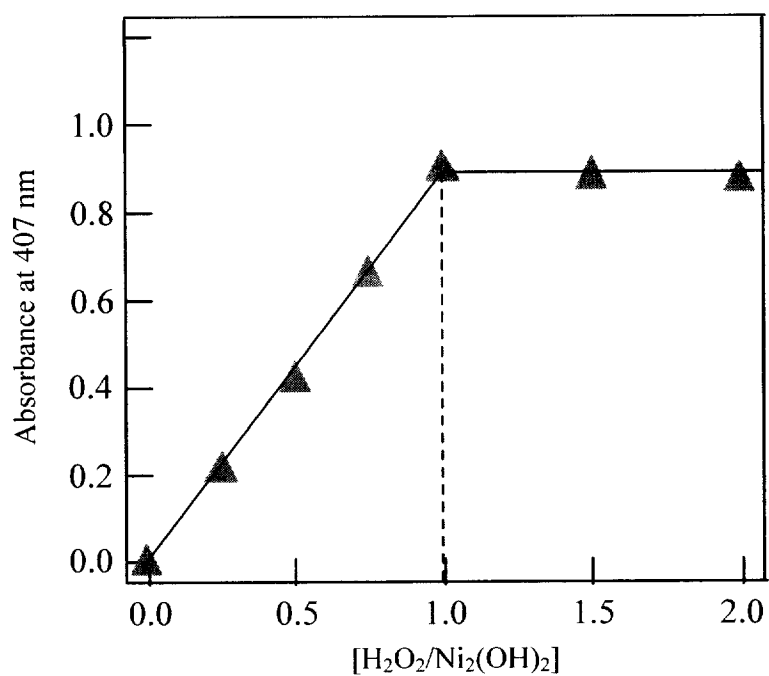
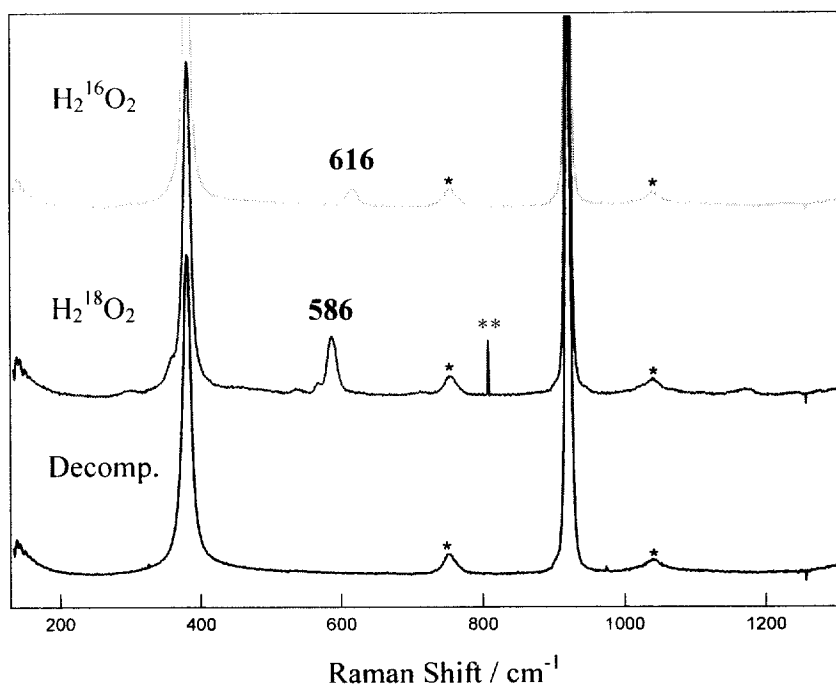**Figure 2.3.** Titration of [Ni$_2$(OH)$_2$(Me$_4$-pyxyl)](ClO$_4$)$_2$ with H$_2$O$_2$ in acetone at

-75 °C.

47

Figure 2.4. Resonance Raman spectra of $[Ni_2(^{16}O)_2(Me_4\text{-pyxyl})]^{2+}$ (upper line) and $[Ni_2(^{18}O)_2(Me_4\text{-pyxyl})]^{2+}$ (lower line) obtained with 406.7 nm excitation in acetone at -40 °C. The "*" mark indicates a solvent band. The "**" mark is not assigned.

3. Results and Discussion

The intense UV-vis band at 407 nm is similar to the characteristic spectra of previously reported bis(μ-oxo)dinickel(III) complexes (Table 2.3). The isotope-sensitive resonance Raman band at 616 cm^{-1} and the observed isotope shift ($\Delta = 30$ cm^{-1}) are also greatly similar to that of the bis(μ-oxo)dinickel(III) complexes. These results clearly indicate the intermediate is a bis(μ-oxo)dinickel(III) complex with formular [Ni$_2$(O)$_2$(Me$_4$-pxyl)]$^{2+}$ (2).

The spectral change in the reaction of 1 and H$_2$O$_2$ is shown in Figure 2.2, where increase of the absorption band at 407 nm obeyed good first-order kinetics (Figure 2.5). The rate constant (k$_f$) of 0.071 s^{-1} at −75°C for the formation of 2 is comparable to that of Itoh's bis(μ-oxo)dinickel(III) complexes (e.g. [Ni$_2$(O)$_2$(L5)]$^{2+}$; k$_f$ = 0.046 s^{-1} at −90°C). Furthermore, the oxygen source of 2 has been confirmed as hydrogen peroxide by the isotope labeling experiment using H$_2$^{18}O$_2$ in the presence of H$_2$^{16}O (Figure 2.4), which implies the existence of a putative (μ-η^2:η^2-peroxo)dinickel(II) species in the formation process. All these results indicate that the formation process for 2 is quite similar to those of Itoh's bis(μ-oxo)dinickel(III) complexes, where a plausible mechanism involving rate-determining isomerization of the bis(μ-hydroxo)dinickel(II) complex prior to a rapid H$_2$O$_2$ attack and fast conversion to the bis(μ-oxo)dinickel(III) complex via a transient (μ-η^2:η^2-peroxo)dinickel(II) species

has been proposed (Scheme 3).

Table 2.3. UV-vis and resonance Raman data for reported bis(μ-oxo)dinickel(III) complexes with tridentate N-donor ligands.

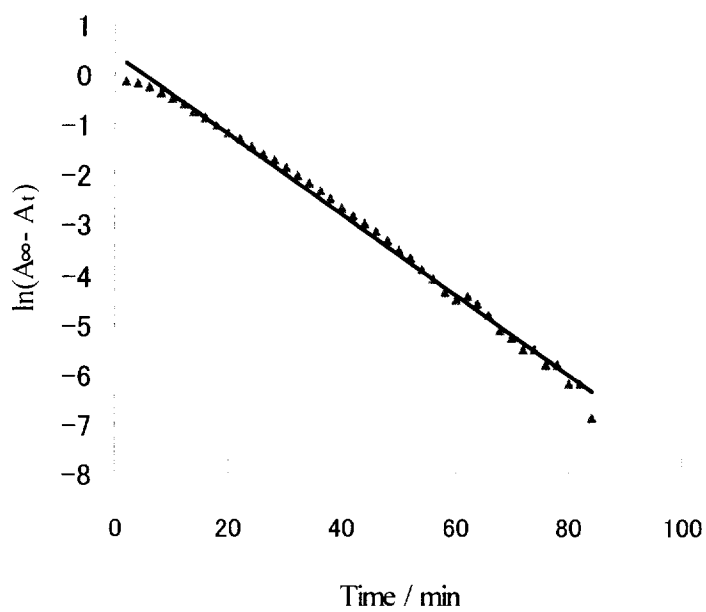| Complex	UV-vis		Raman			ref.
	λ_{max} / nm	ε / M^{-1} cm^{-1}	ν (^{16}O)	ν (^{18}O)	$\Delta\nu$	
[Ni$_2$(O)$_2$(L1^H)]$^{2+}$	408	6000	612	580	32	[13]
[Ni$_2$(O)$_2$(L2)]$^{2+}$	406	3000	616, 600	578, 568	32, 32	[13]
[Ni$_2$(O)$_2$(L3)]$^{2+}$	412	4800	599	570	29	[13]
[Ni$_2$(O)$_2$(L4)]$^{2+}$	414	5600	609	579	30	[13]
[Ni$_2$(O)$_2$(L5)]$^{2+}$	406	1200	610	577	33	[13]
[Ni$_2$(O)$_2$(Tp^{Me3})]$^{2+}$	410	4200				[14]
[Ni$_2$(O)$_2$(Tp^{Me2})]$^{2+}$	405	3900				[14]
[Ni$_2$(O)$_2$(Tp^{Me2,Br})]$^{2+}$	404	2800				[14]
[Ni$_2$(O)$_2$(Tp^{iPr2})]$^{2+}$	404	10500				[14]

Figure 2.5. First-order plot based on the absorption change at 407 nm.
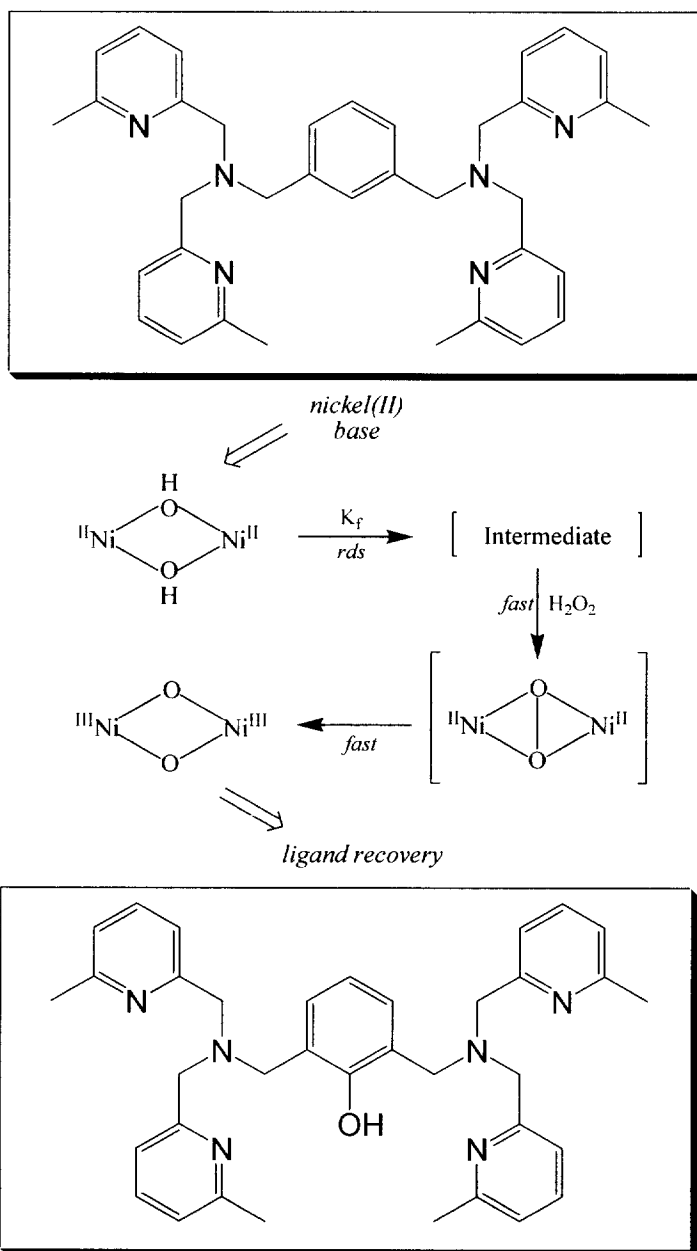
Scheme 3.

Complex **2** is relatively stable at low temperature (below $-70°C$), whereas decomposition gradually occurs at high temperature (above $-30°C$), leading to arene hydroxylation, as those to be observed in the reaction of $[Cu_2(Me_4\text{-pyxyl})]^{2+}$ with O_2. The ESI-TOF/MS spectrum of the thermally decomposed solution shows a prominent signal at *m/z* 352, whose masses and observed isotope patterns were consistent with their respective formulation as $[Ni_2(OH)(Me_4\text{-pyxyl-O})]^{2+}$ **(3)** (Figure 2.6.). The formation of Me$_4$-pyxyl-OH was also confirmed by a ligand-recovery experiment using ^{1}H-NMR (Figure 2.7); the yield of arene hydroxylation (Me$_4$-pyxyl-OH) was 72 %. The oxygen source for the phenoxo group in Me$_4$-pyxyl-OH was identified as hydrogen peroxide by the isotope labeling experiment using $H_2^{18}O_2$ (Figure 2.4), indicating that the arene hydroxylation involves oxygen transfer from the bis(μ-oxo)dinickel(III) core in **2**, as observed in arene hydroxylation by Cu system .
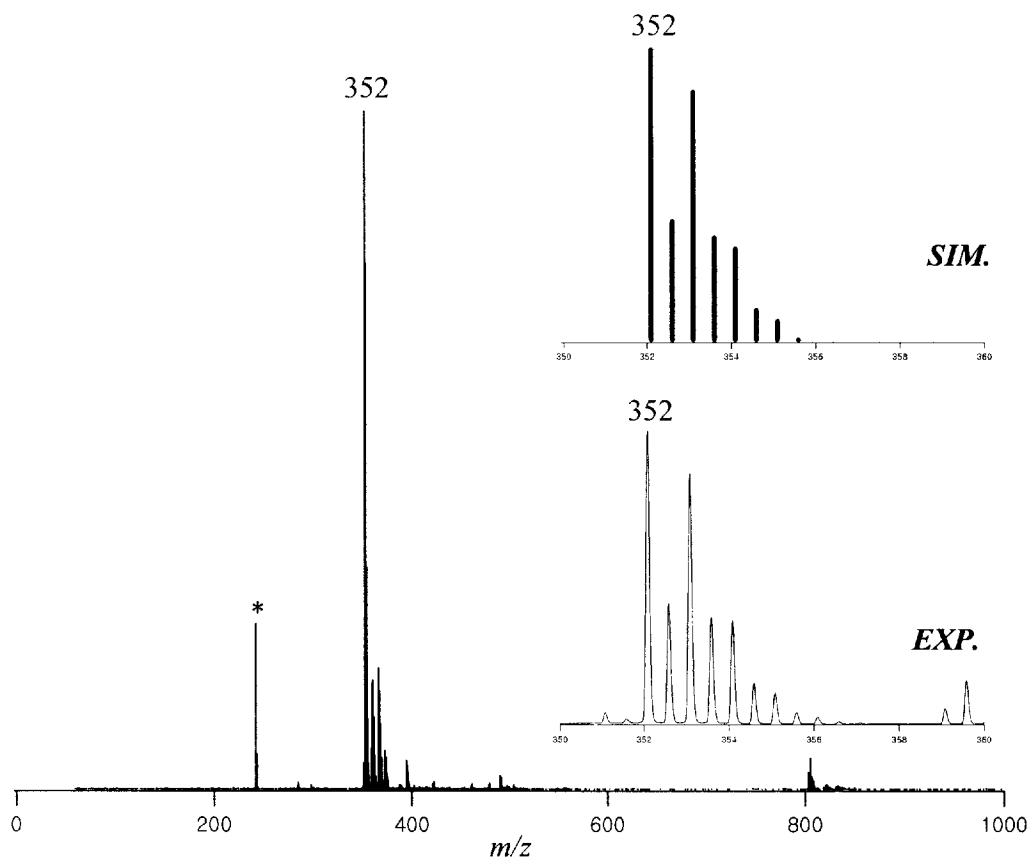
Figure 2.6. ESI-TOF/MS spectrum of a thermally decomposed solution of **2**. Insets are the experimental spectrum (lower) in the m/z 350 - 360 region and the simulated one (upper) showing the formation of arene hydroxylation, $[\{Ni_2(OH)(Me_4\text{-pyxyl-O})\}^{2+}]$ (m/z 352). Asterisk (*) shows a reference mark ($[\{CH_3(CH_2)_3\}_4N^+]$: m/z 242.2848).

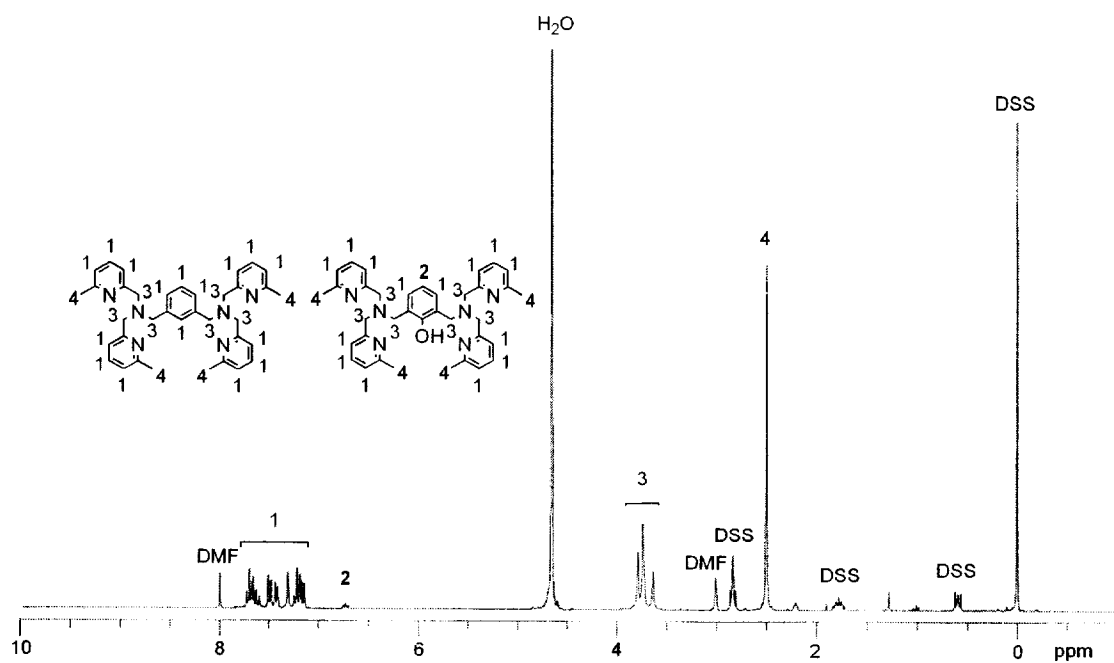**Figure 2.7.** ^{1}H-NMR spectrum for the product of thermal decomposition of **2** in

[D$_7$]DMF/D$_2$O in the presence of NaCN.

In conclusion, we have demonstrated the first example of arene hydroxylation by a bis(μ-oxo)dinickel(III) core, in sharp contrast to the result that all previously reported bis(μ-oxo)dinickel(III) cores have activated an aliphatic C-H bond. It is noteworthy that a bis(μ-oxo)dinickel(III) core is produced as an intermediate for arene hydroxylation reaction, in contrast with Cu system, which forms a (μ-η^2:η^2-peroxo)dicopper(II) core with the same ligand. Previous spectroscopic and computational studies on a related bis(μ-oxo)dinickel(III) core show significant kinetic and thermodynamic stability for the bis(μ-oxo)dinickel(III) core relative to a putative (μ-η^2:η^2-peroxo)dinickel(II) core. Thus this Ni system, unlike Cu system, clearly shows a bis(μ-oxo) core is able to hydroxylate an arene directly.

4. References

[1]   (a) Solomon, E. I.; Sundaram, U. M.; Machonkin, T. E. *Chem. Rev.* **1996**, *96*, 2563. (b) Que, L., Jr.; Tolman, W. B. *Angew. Chem. Int. Ed.* **2002**, *41*, 1114. (c) Lewis, E. A.; Tolman, W. B. *Chem. Rev.* **2004**, *104*, 1047. (d) Solomon, E. I.; Chen, P.; Metz, M.; Lee, S.; Palmer, A. E. *Angew. Chem. Int. Ed.* **2001**, *40*, 4570.

[2]   (a) Karlin, K. D.; Hayes, J. C.; Gultneh, Y.; Cruse, R. W.; McKown, J. W.; Hutchinson, J. P.; Zubieta, J. *J. Am. Chem. Soc.* **1984**, *106*, 2121. (b) Karlin, K. D.; Nasir, M. S.; Cohen, B. I.; Cruse, R. W.; Kaderli, S.; Zuberbühler, A. D. *J. Am. Chem. Soc.* **1994**, *116*, 1324. (c) Mahapatra, S.; Karderli, S.; Llobet, A.; Neuhold, Y.-M.; Palanché, T.; Halfen, J. A.; Young, V. G, Jr.; Kaden, T. A.; Que, L., Jr.; Zuberbühler, A. D.; Tolman, W. B. *Inorg. Chem*, **1997**, *36*, 6343. (d) Pidcock, E; Obias, H. V.; Zhang, C. X.; Karlin, K. D.; Solomon, E. I. *J. Am. Chem. Soc.* **1998**, *120*, 7841.

[3]   Holland. P. L.; Rodgers, K. R.; Tolman, W. B. *Angew. Chem. Int. Ed.* **1999**, *38*, 1139.

[4]   Mirica, L. M.; Vance, M.; Rudd, D. J.; Hedman, B.; Hodgson, K. O.; Solomon, E. I.; Stack, T. D. P. *Science*, **2005**, *308*, 1890.

[5]   (a) Cramer, C. J.; Smith, B. A.; Tolman, W. B. *J. Am. Chem. Soc.* **1996**, *118*,

11283. (b) Bérces, A. *Inorg. Chem*, **1997**, *36*, 4831. (c) Flock, M.; Pierloot, K. *J. Phys. Chem. A* **1999**, *103*, 95. (d) Henson, M. J.; Mukherjee, P.; Root, D. E.; Stack, T. D. P.; Solomon, E. I. *J. Am. Chem. Soc.* **1999**, *121*, 10332.

[6]   Schenker, R.; Mandimutsira, B. S.; Riordan, C. G.; Brunold, T. C. *J. Am. Chem. Soc.* **2001**, *124*, 13842.

[7]   (a) Kimura, E.; Sakonaka, A.; Machida, R. *J. Am. Chem. Soc.* **1982**, *104*, 4255. (b) Kimura, E.; Machida, R. *J. Chem. Soc., Chem. Commun.* **1984**, 499. (c) Kimura, E.; Machida, R.; Kodama, M. *J. Am. Chem. Soc.* **1984**, *106*, 5497. (d) Kushi, Y.; Machida, R.; Kimura, E. *J. Chem. Soc., Chem. Commun.* **1985**, 216.

[8]   Reported bis(μ-oxo)Ni$_2^{III}$ complexes: Hikichi's complexes (a) Hikichi, S.; Yoshizawa, M.; Sasakura, Y.; Komatsuzaki, H.; Moro-oka, Y.; Akita, M. *Chem. Eur. J.* **2001**, *7*, 5012. Itoh's complexes (b) Itoh, S.; Bandoh, H.; Nakagawa, M.; Nagatomo, S.; Kitagawa, T.; Karlin, K. D.; Fukuzumi, S. *J. Am. Chem. Soc.* **2001**, *123*, 11168. Suzuki's complex (c) Shiren, K.; Ogo, S.; Fujinami, S.; Hayashi, H.; Suzuki, M.; Uehara, A.; Watanabe, Y.; Moro-oka, Y. *J. Am. Chem. Soc.* **2000**, *122*, 254. Riordan's complex (d) Mandimutsira, B. S.; Yamarik, J. L.; Brunold, T. C.; Gu, W.; Cramer, S. P.; Riordan, C. G.; *J. Am. Chem. Soc.* **2001**, *123*, 9194.

[9]   An unpublished work by Matsumoto

[10]   *SIR-92*: Altomare, A.; Cascarano, G.; Giocovazzo, C.; Guagliardi, A.; Burla,

        M. C.; Ploidori, G.; Camalli, M. J. Appl. Crystallogr. **1994**, *27*, 435.

[11]   Beurskens, P. T.; Admiraal, G.; Beurskens, G.; Bosman, W. P.; de Gelder, R.;

        Israel, R.; Smits, J. M. M. *The DIRDIF-94 program system* (1994), Technical

        Report of the Crystallography Laboratory: University of Nijmegen:

        Nijmegen, The Netherlands, 1994.

[12]   *teXsan*: Crystal Structure Analysis Package, Molecular Structure

        Corporation: The Woodlands, TX. 1985 and 1992.

[13]   Itoh, S.; Bandoh, H.; Nakagawa, M.; Nagatomo, S.; Kitagawa, T.; Karlin, K.

        D.; Fukuzumi, S. *J. Am. Chem. Soc.* **2001**, *123*, 11168.

[14]   Hikichi, S.; Yoshizawa, M.; Sasakura, Y.; Komatsuzaki, H.; Moro-oka, Y.;

        Akita, M. *Chem. Eur. J.* **2001**, *7*, 5012.

Korean Abstract

3,14-dimethyl-2,6,13,17-tetraazatricyclo[14.4.0^{1,18}.0^{7,12}]docosane ligand (L)를 갖는 두 개의 새로운 구리(II) 착화합물을 합성하고 X-ray 회절법에 의해서 구조적인 특성을 확인하였다. 첫 번째 착화합물 [Cu(L1)]·(ClO$_4$)$_2$ (1)에서 리간드의 형태는 평면이고, 두 개의 unidentate ClO$_4^-$ 이온에 의해서 구리 이온에 대해 정팔면체 구조를 취하고 있다. 두 번째 착화합물 [Cu(L2)(O$_2$CH)]·ClO$_4$ (2)에서 구리 원자에 대한 배위 형태는 거대 고리로부터의 4개의 수평방향의 질소 원자와 formate 리간드로부터의 산소 원자, 그리고 배위되지 않은 ClO$_4^-$ 이온에 의해 독특한 square pyramid를 취하고 있다. 두 개의 착화합물에서 다양한 형태의 수소결합 상호작용은 구리(II) 이온 주위의 형태를 결정하는데 중요한 역할을 한다.

Me$_4$-pyxyl 리간드를 갖는 bis(μ–oxo)dinickel(III) 화합물은 bis(μ–oxo)dinickel(III) core 에 의해서 arene hydroxylation의 반응성을 보인다. bis(μ–oxo)dinickel(III) core는 저온에서 bis(μ–hydroxo)dinickel(II) 화합물과 같은 당량의 H$_2$O$_2$에 의해서 성공적으로 발생된다. bis(μ–oxo)dinickel(III) 화합물은 407 nm에서 특징적인 UV-vis 흡수띠를 나타내고, 616 cm^{-1} 에서 resonance Raman 띠는 ^{18}O-치환 하에서 586 cm^{-1} 로 이동한다. 반응속도론적 연구와 H$_2$^{18}O$_2$ 를 사용한 isotope labeling 실험은 bis(μ–oxo)dinickel(III) 화합물의 형성과정에 peroxo dinickel(II)와 같은 중간체의 존재를 암시한다. bis(μ–oxo)dinickel(III) 화합물을 차츰 분해시키면 리간드의 arene ring이 hydroxylation된다. Isotope labeling 실험은 phenoxo group의 산소 source는 H$_2$O$_2$라는 것을 나타내고 이것은 arene hydroxylaation이 bis(μ–oxo)dinickel(III) core로부터의 산소 이동을 포함한다는 것을 보여준다. 구리 계에서 유사한 arene hydroxylation에서는 같은 리간드를 가지는 ($\mu-\eta^2:\eta^2-$peroxo)dicopper(II) 화합물이 중간체로써 관찰된다. 니켈과 구리 계 사이에서 활성 산소 화합물의 구조와 반응성에 대한 비교가 논의 되었다.

Acknowledgments

I would like to express my sincere gratitude to Professor Ju Chang Kim for his considerate guidance and continuous encouragement in the course of this thesis. I express my special thanks to Pukyong National University (PKNU), which gave me a wonderful chance to study at Kanazawa University in Japan.

I would also like to thank Professors Don Kim and Yong Cheol Kang for their time and comments for this thesis. I am appreciative of the guidance and help of other faculties during the stay at department of chemistry at PKNU. In addition, I am grateful to Prof. Alan J. Lough (University of Toronto, Chapter I), Prof. Shuhei Fujinami (Kanazawa University, Chapter II) for solving X-ray crystallographic data, I also thanks to Prof. Teizo Kitagawa and Dr. Takehiko Tosha (Okazaki National Research Institutes) for much appreciated advice throughout the resonance Raman spectroscopy.

Also, I would like to appreciate the effort of Professors Masatatsu Suzuki, Shuhei Fujinami, and Hideki Hurutachi for teaching me how to research the works in Chapter II, and providing the life in Japan as an international exchange student for a year.

I specially thank to Dr. Jaeheung Cho for his kind derection during the stay at the Kanazawa University, and I want to thank for the hospitality of my colleagues,